

This is the preprint of the contribution published as:

Burot, C., Amiraux, R., Bonin, P., Guasco, S., Babin, M., Joux, F., Marie, D., Vilgrain, L., **Heipieper, H.J.**, Rontani, J.-F. (2021):

Viability and stress state of bacteria associated with primary production or zooplankton-derived suspended particulate matter in summer along a transect in Baffin Bay (Arctic Ocean) *Sci. Total Environ.* **770** , art. 145252

The publisher's version is available at:

<http://dx.doi.org/10.1016/j.scitotenv.2021.145252>

1
2
3 Viability and stress state of bacteria associated with
4 primary production or zooplankton-derived suspended
5 particulate matter in summer along a transect in Baffin
6 Bay (Arctic Ocean)

7
8 Christopher Burot^a, Rémi Amiraux^{a,b,c}, Patricia Bonin^a, Sophie Guasco^a, Marcel
9 Babin^c, Fabien Joux^d, Dominique Marie^e, Laure Vilgrain^f, Hermann Heipieper^g,
10 Jean-François Rontani^{a*}

11
12
13
14 ^a Aix-Marseille University, Université de Toulon, CNRS/INSU/IRD, Mediterranean Institute
of Oceanography (MIO), UM 110, 13288 Marseille, France.
15 ^b UMR 6539 Laboratoire des Sciences de l'Environnement Marin (CNRS, UBO, IRD, Ifremer)
16 Institut Universitaire Européen de la Mer (IUEM) Plouzané, France.
17 ^c Takuvik Joint International Laboratory, Laval University (Canada) - CNRS, Département de
18 biologie, Université Laval, Québec G1V 0A6, Québec, Canada.
19 ^d Sorbonne Université, CNRS, Laboratoire d'Océanographie Microbienne (LOMIC),
20 Observatoire Océanologique de Banyuls, 66650 Banyuls sur mer, France.
21 ^e Sorbonne Université, CNRS, UMR 7144, Station Biologique de Roscoff, 29680 Roscoff,
22 France.
23 ^f Sorbonne Université, CNRS UMR 7093, LOV, Observatoire océanologique, Villefranche-sur-
24 Mer, France.
25 ^g Department of Environmental Biotechnology, Helmholtz Centre for Environmental Research
26 – UFZ, Permoserstr. 15, 04318 Leipzig, Germany.

29 * Corresponding author. Tel.: +33-4-86-09-06-02; fax: +33-4-91-82-96-41. E-mail address:
30 jean-francois.rontani@mio.osupytheas.fr (J.-F. Rontani)

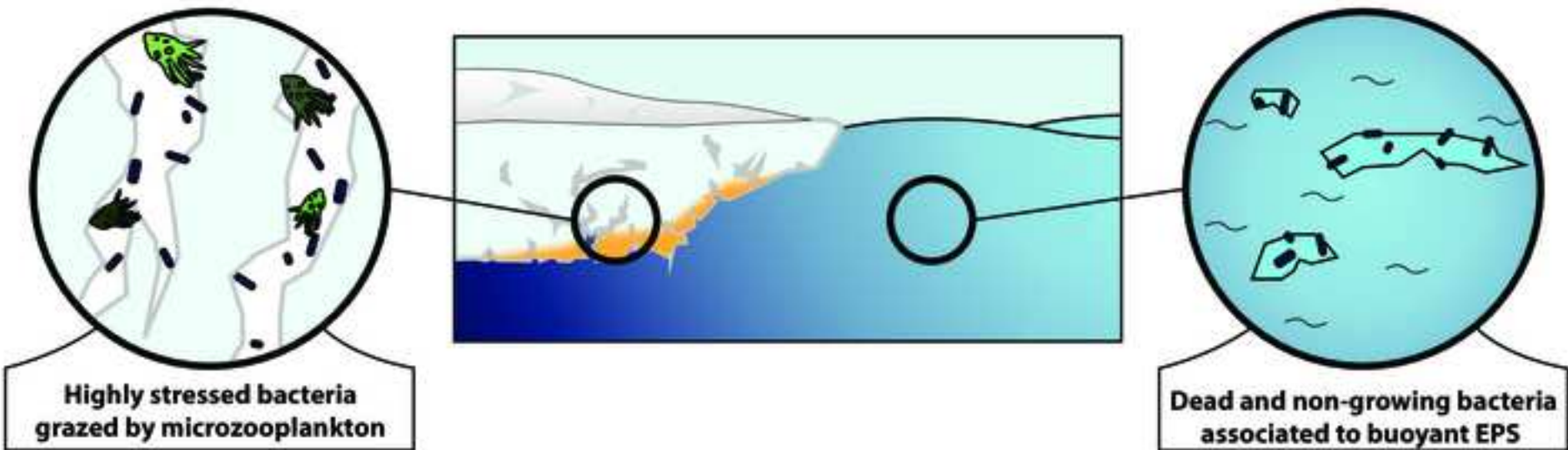
31 **Abstract**

32 In the framework of the GreenEdge Project (whose the general objective is to understand the
33 dynamic of the phytoplankton spring bloom in Arctic Ocean), lipid composition and viability
34 and stress state of bacteria were monitored in sea ice and suspended particulate matter (SPM)
35 samples collected in 2016 along a transect from sea ice to open water in Baffin Bay (Arctic
36 Ocean). Lipid analyses confirmed the dominance of diatoms in the bottommost layer of ice and
37 suggested (i) the presence of a strong proportion of micro-zooplankton in SPM samples
38 collected at the western ice covered St 403 and St 409 and (ii) a high proportion of macro-
39 zooplankton (copepods) in SPM samples collected at the eastern ice covered St 413 and open
40 water St 418. The use of the propidium monoazide (PMA) method allowed to show a high
41 bacterial mortality in sea ice and in SPM material collected in shallower waters at St 409 and
42 St 418. This mortality was attributed to the release of bactericidal free fatty acids by sympagic
43 diatoms under the effect of light stress. A strong *cis-trans* isomerization of bacterial MUFAs
44 was observed in the deeper SPM samples collected at the St 403 and St 409. It was attributed
45 to the ingestion of bacteria stressed by salinity in brine channels of ice by sympagic
46 bacterivorous microzooplankton (ciliates) incorporating *trans* fatty acids of their preys before
47 to be released in the water column during melting. The high *trans/cis* ratios also observed in
48 SPM samples collected in the shallower waters at St 413 and St 418 suggest the presence of
49 positively or neutrally buoyant extracellular polymeric substances (EPS)-rich particles retained
50 in sea ice and discharged (with bacteria stressed by salinity) in seawater after the initial release
51 of algal biomass. Such EPS particles, which are generally considered as ideal vectors for
52 bacterial horizontal distribution in the Arctic, appeared to contain a high proportion of dead and
53 non-growing bacteria.

54

55

56 **Keywords:** Sea ice algae; Bacterial viability; Salinity stress; *Cis-trans* isomerase; EPS; Micro-
57 and macro-zooplankton.



- Grazing of salinity-stressed bacteria by microzooplankton in brine channels of ice
- Incorporation of the dietary bacterial isomerized fatty acids by microzooplankton
- Induction of high bacterial mortality by free fatty acid producing ice algae
- Dead or non-growing bacteria associated to buoyant EPS particles in surface waters
- Good viability of bacteria associated to zooplanktonic material in deeper waters

58
59

1. Introduction

60 Arctic sea ice shelters a huge diversity of organisms particularly well-adapted to the harsh
61 living conditions in this ecosystem (Boetius et al., 2015). They include bacteria, viruses, archaea
62 and diatoms (von Quillfeldt et al., 2003; Junge et al., 2004; Sazhin et al., 2018). One of the
63 numerous ecosystem services that this particular biota fulfil is the production of organic matter
64 (Boras et al., 2010; Boetius et al., 2015). Sympagic diatoms (diatoms inhabiting the ice matrix)
65 are responsible for much of this production. Their contribution to annual primary production
66 (PP) varies widely depending on the season and the region (<1–60%, e.g. Dupont, 2012;
67 Fernández-Méndez et al., 2015), but it represents a crucial food source for the marine food web,
68 especially in winter (Søreide et al., 2010).

69 It has been shown that Arctic sea ice contains large amounts of extracellular polymeric
70 substances (EPSs) (Krembs et al., 2002), one order of magnitude higher than in the surface
71 water (Krembs and Engel, 2001; Meiners et al., 2003). These substances are produced by both
72 bacteria and algae, with sympagic diatoms being their primary source in sea ice (Meiners et al.,
73 2003; Mancuso Nichols et al., 2004). EPSs can help protect cells against harsh environmental
74 conditions (e.g. salinity fluctuations) and assist cell adhesion (Cooksey and Wigglesworth-
75 Cooksey, 1995). The release of exopolymers by the sympagic biota further influences carbon
76 cycling by (i) providing a carbon-rich substrate that will support bacterial production and
77 metabolic activity (Simon et al., 2002), (ii) bypassing microbially mediated POC production by
78 the abiotic formation of large EPS-containing particles or aggregates (Passow, 2002; Thornton,
79 2002), (iii) directly contributing to the organic carbon pool, with concentrations potentially
80 equivalent to those of particulate organic carbon (POC) in pelagic environments (Mari, 1999;
81 Engel and Passow, 2001), and (iv) increasing the sympagic biota sedimentation rates through
82 aggregation (Riebesell et al., 1991; Azetsu-Scott and Passow, 2004). From their high
83 sedimentation rates and their good preservation during their travel toward the seafloor (Boetius

84 et al., 2013; Rontani et al., 2016; Amiraux et al., 2017), it has been suggested that sympagic PP
85 contributes significantly to the total PP source in sea waters, especially deep ones (Glud and
86 Rysgaard, 2007; Krause-Jensen et al., 2007). The fate of sympagic biota in sea ice and as they
87 sink in the water column depends mostly on grazing by zooplankton and mineralization by their
88 attached bacteria. In the Arctic, it is estimated that the zooplankton graze about 66–79% of the
89 new PP (including sympagic algae; Forest et al., 2011), and since their fecal pellets generally
90 increase the sinking rates of their food, it is estimated that zooplankton probably form most of
91 the PP export to the aphotic zone and seafloor (Forest et al., 2011). By contrast, bacterial
92 activity, which is higher for attached than for free bacteria (Hoppe, 1991; Karner and Herndl,
93 1992), allows cleavage of the POM into smaller pieces by extracellular enzymatic hydrolysis
94 (Cho and Azam, 1988). Such processes enhance the further enzymatic digestion of the matter
95 and ultimately reduce its potential to reach the seafloor. However, while heterotrophic bacteria
96 and the rest of the microbial loop process about half of the PP in low-latitude oceans (Ducklow,
97 2000), their contribution at higher latitudes is assumed to be smaller. Based on bacterial activity
98 measurements, Howard-Jones et al. (2002) suggest that a significant fraction (25–80%) of
99 Arctic bacterioplankton is dormant or inactive in the marginal ice zone of the Barents Sea.

100 Recently, Amiraux et al. (2017) suggested that the weaker activity of bacteria in the
101 Arctic could result from the involvement of some stress factors in ice, such as salinity. During
102 the early stage of ice melting in spring, brine inclusions (where salinity may reach up to 150 in
103 some ice sections collected in early spring 2015 at the GreenEdge Ice Camp, Galindo,
104 unpublished data) become interconnected in channels and are expelled from the sea ice into the
105 underlying seawater (Wadhams and Martin, 2001). The ice algal bacterial community is
106 therefore exposed to a salinity stress, which occurs over relatively short timescales (e.g. hours).
107 In this ecosystem, prokaryotic cells subjected to high osmotic pressure have developed
108 mechanisms to live in these extreme conditions. Various strategies are used: (i) implementation

109 of active Na⁺ and K⁺ ion transport systems (Thompson and MacLeod, 1971), (ii) accumulation
110 of osmocompatible compounds such as glycine betaine or proline (Piuri et al., 2003) or (iii)
111 production of EPSs, which can act as a diffusion barrier (Kim and Chong, 2017). Another major
112 adaptive response of many microorganisms, including bacteria, is to maintain membrane
113 fluidity through ‘homeoviscous adaptation’ (Sinensky, 1974). The shifts in fatty acid
114 composition of membrane lipids, and most notably by enzymatic conversion of *cis*- to *trans*-
115 unsaturated fatty acids (Loffeld and Keweloh, 1996; Heipieper et al., 2003) through the activity
116 of *cis-trans* isomerases (CTIs) can be an important bacterial mechanism for modifying
117 membrane fluidity. It has been previously suggested that *trans/cis* ratios > 0.1 in environmental
118 samples may be indicative of bacterial stress (Guckert et al., 1986). Previous analyses of sea
119 ice and sinking particles collected in the water column during the vernal melting period showed
120 a relatively strong CTI activity, suggesting the occurrence of salinity stress during the early
121 stages of ice melt (Amiriaux et al., 2017). The high *trans/cis* ratios observed in sinking particles
122 was attributed to the flush of bacteria associated with ice algae from internal hypersaline ice
123 brines (Amiriaux et al., 2021b). The relative stability of these ratios with depth also suggested
124 that bacterial communities associated with sinking sympagic algae were non-growing.

125 In a previous study, Amiriaux et al. (2021a) studied the stress state of bacteria attached to
126 sinking sympagic algae during a vernal melting season at a landfast ice station in Davis Strait.
127 Their results emphasized the impact of salinity, limiting the growth state of attached bacteria at
128 the beginning of sea ice melting, subsequently giving way to an intense free fatty acid (FFAs)
129 stress. Indeed, the production of bactericidal FFAs by sympagic algae is enhanced by the
130 increase in light transmittance through the ice (due to the advance melting of sea ice) resulting
131 in a high bacterial mortality. If this study gave us valuable information on the interactions
132 between sympagic algae and their associated bacteria in sinking samples, data on those
133 interactions after ice melting and on suspended particles are still lacking.

134 In the present work, we thus monitored the salinity stress and mortality of bacteria
135 associated with sea ice and suspended particulate matter (SPM) samples collected in 2016 along
136 a transect from sea ice to open water in Baffin Bay (Arctic Ocean). We intend to determine if
137 the bacteria associated with these suspended particles are also weakly active or in a poor
138 physiological state, thus impacting the preservation of this material.

139

140 **2. Materials and methods**

141

142 *2.1. Sampling*

143 Samples were taken at three ice stations (St 403, St 409 and St 413) and one open water
144 station (St 418) (Fig. 1) from the Canadian icebreaker CCGS *Amundsen* along a longitudinal
145 transect from 68° 4' 25.32"N and 61° 36' 30.54" W to 68° 6' 52.14" N and 57° 46' 7.14" W
146 between 25 and 28 June 2016 as part of the GreenEdge project. At the time of sampling, this
147 transect was under the influence of the Arctic current from the North acting practically
148 perpendicular to the transect (A. Randelhoff, Personal communication). Consequently,
149 advection along the transect (East-West) should be relatively limited.

150 The sea ice sampling was carried out using a Kovacs Mark V 14 cm diameter corer,
151 focusing on the bottom-most 10 cm of sea ice (sub-sectioned into two further intervals: 0–3 and
152 3–10 cm) where most ice biota are found (Smith et al., 1990). To compensate for biomass
153 heterogeneity, common in sea ice (Gosselin et al., 1986), three or four equivalent core sections
154 were pooled for each sampling day in isothermal containers. Pooled sea ice sections were then
155 melted in the dark with 0.2 µm filtered seawater (FSW; 3:1 v:v) to minimize osmotic stress on
156 the microbial community during melting (Bates and Cota, 1986; Garrison and Buck, 1986).

157 Suspended particulate matter (SPM) samples were collected at seven depths in the first
158 100 m of the water column using large (20 L) Niskin bottles to accommodate any within-sample
159 heterogeneity.

160 For both sea ice and SPM, samples were collected in pentaplicate (a sample for lipid
161 analyses and four for PMA analyses) as follows. Lipid, chlorophyll *a*, and total particulate
162 carbon samples were obtained by filtration through pre-weighed Whatman glass fiber filters
163 (Buckinghamshire, UK; GF/F, porosity 0.7 μm , combusted 4 h at 450°C) and kept frozen (< -
164 80°C). Bacterial viability samples were obtained by filtration on 0.8 μm Whatman nucleopore
165 filters (24 mm, autoclaved 1 h at 110°C) and kept frozen (< -80°C) prior to analysis. Owing to
166 the porosity of the filters, the analyses concerned mainly algae, particles and their attached
167 bacteria. Bacterial abundance and productivity were measured directly onboard the CCGS
168 *Amundsen* by cytometry (see *Bacterial abundance*) and ^3H -leucine incorporation (see *Bacterial*
169 *productivity*).

170

171 2.2. Treatment

172

173 2.2.1. Chlorophyll *a*

174 Concentration of chlorophyll *a* and phaeopigments retained on the GF/F filters were
175 measured before and after acidification (5% HCl) using a TD-700 Turner Design fluorometer,
176 after 18–24 h extraction in 90% acetone at 4°C in the dark (Parsons et al., 1984). The
177 fluorometer was calibrated with a commercially available chlorophyll *a* standard (*Anacystis*
178 *nidulans*, Sigma).

179

180 2.2.2. Total particulate carbon

181 At Université Laval, filters were dried for 24 h at 60°C, weighed again for dry weight
182 determination and then analyzed using a Perkin Elmer carbon-hydrogen-nitrogen-sulfur
183 (CHNS) 2400 Series II instrument to measure TPC. Calibration was done using accurately
184 weighed samples of acetanilide (C₈H₉NO).

185

186 2.2.3. *Bacterial abundance*

187

188 Samples were analyzed directly on board the CCGS *Amundsen* using an Accuri C6 flow
189 cytometer equipped with 488 nm and 633 nm lasers and the standard filter setup. For
190 enumeration of phototrophs, cells were detected on the base of their red fluorescence (FL3) and
191 unfixed samples were analyzed 3 min at a flow rate around 65 µL min⁻¹. Samples were then
192 fixed with 0.25% glutaraldehyde (final concentration) and stained for a minimum of 15 min
193 with SYBR Green I at 1/10 000 of the commercial solution for enumeration of heterotrophic
194 cells (Marie et al. 1999). Trigger was set on the green fluorescence of the SYBR and samples
195 were analyzed 2 min at a flow rate of about 35 µL min⁻¹.

196

197 2.2.4. *Bacterial productivity*

198 Bacterial production (BP) was measured for 8 to 10 depths per station, distributed in the
199 first 350 m, by [³H]-leucine incorporation (Kirchman et al., 1985) modified for
200 microcentrifugation (Smith and Azam, 1992). Triplicate 1.7 mL aliquots were incubated with
201 a mixture of 50/50 (v/v) [³H]- leucine (Perkin Elmer) and nonradioactive leucine for 4 h at a
202 temperature (1.5°C) close to that *in situ*. Samples with 5% trichloroacetic acid added prior to
203 the isotope served as blank. Saturation and time course were performed beforehand to determine
204 the concentration of leucine and minimum incubation time. Leucine incorporation was
205 converted to carbon production using a conservative conversion factor of 1.5 kg C mol⁻¹ leucine
206 (Simon and Azam, 1989).

207

208 2.2.5. Bacterial viability analysis

209 The bacterial viability analysis was conducted using a method based on propidium
210 monoazide (PMA). PMA is a photoreactive dye that binds to DNA, inhibiting its replication by
211 PCR. Live cells have intact membranes and are impermeable to PMA, which only influxes into
212 cells with disrupted membranes. The combination of PMA use and PCR provides a rapid and
213 reliable method for discriminating live and dead bacteria. The viability analysis requires two
214 sets of the same sample, one treated with PMA (that gives the quantity of living organisms in
215 the sample) and an untreated one (that gives the total amount of organisms in the sample).

216 The first step of this method consists of a treatment of the concentrated and filtrated
217 samples with PMA, the filters are then exposed to light, allowing PMA to bind with DNA. For
218 a detailed protocol see Amiraux et al. (2021a).

219 Nucleic acids were extracted using a chloroform-based method. Filters were placed in
220 2 mL Eppendorf[®] tubes and heat-shocked (+80°C then -80°C alternately, twice) to improve
221 cell lysis. 100 µL of lysis solution (Tris 20 mM, EDTA 25 mM, lysozyme 1 µg.µL⁻¹) was added
222 and the samples were incubated at 37°C for 15 min. 900 µL of sterile ice-cold water and 900 µL
223 of chloroform were then added and the samples were vortexed five times for 5 s and then
224 centrifuged for 5 min at 10,000 × g. 700 µL of the aqueous phase was collected, transferred to
225 a new tube and any traces of remaining chloroform removed in speed vacuum concentrator
226 (Savant DNA 120, Thermo Scientific[™]) for 15 min. Finally, 10 µL of RNase (10 mg. mL⁻¹)
227 was added to the samples, and they were incubated for 30 min at 37°C or overnight at 4°C. The
228 DNA obtained was kept frozen at -20°C for further use.

229 Absolute quantification of bacterial SSU ribosomal RNA (rRNA) gene was carried out
230 by qPCR with SsoAdvanced[™] Sybr Green Supermix on a CFX96 Real-Time System (C1000

231 Thermal Cycler, Bio-Rad Laboratories, CA, USA) according to the procedure described in
232 Fernandes et al. (2016). For more details about the qPCR program, see Amiraux et al. (2021a).

233

234 2.2.6. Lipid extraction

235 Samples (GF/F filters) were reduced with excess NaBH₄ after adding MeOH (25 mL,
236 30 min) to reduce labile hydroperoxides (resulting from photo- or autoxidation) to alcohols,
237 which are more amenable to analysis using gas chromatography-mass spectrometry (GC-MS).
238 Water (25 mL) and KOH (2.8 g) were then added and the resulting mixture saponified by
239 refluxing (2 h). After cooling, the mixture was acidified (HCl, 2 N) to pH 1 and extracted with
240 dichloromethane (DCM; 3 × 20 mL). The combined DCM extracts were dried over anhydrous
241 Na₂SO₄, filtered and concentrated by rotary evaporation at 40°C to give total lipid extracts
242 (TLEs). Aliquots of TLEs were either silylated and analyzed by gas chromatography-electron
243 impact quadrupole time-of-flight mass spectrometry (GC-QTOF) for sterol quantification, or
244 methylated, and then treated with dimethyldisulfide (DMDS) and analyzed by GC-MS/MS for
245 the determination of monounsaturated fatty acid double-bond stereochemistry as previously
246 described by Amiraux et al. (2017). *Cis* and *trans* isomers of monounsaturated fatty acid
247 (MUFA) methyl esters react with DMDS, stereospecifically, to form *threo* and *erythro* adducts,
248 which exhibit similar mass spectra but are well-separated by gas chromatography, allowing
249 unambiguous double-bond stereochemistry determination (Buser et al., 1983).

250

251 2.2.7. Gas chromatography-tandem mass spectrometry

252 GC-MS and GC-MS/MS analyses were performed using an Agilent 7890A/7010A
253 tandem quadrupole gas chromatograph system (Agilent Technologies, Parc Technopolis - ZA
254 Courtaboeuf, Les Ulis, France). A cross-linked 5% phenyl-methylpolysiloxane (Agilent; HP-
255 5MS ultra inert, 30 m × 0.25 mm, 0.25 µm film thickness) capillary column was used. Analyses

256 were performed with an injector operating in pulsed splitless mode set at 270°C. Oven
257 temperature was ramped from 70°C to 130°C at 20°C min⁻¹, then to 250°C at 5°C min⁻¹ and
258 then to 300°C at 3°C min⁻¹. The pressure of the carrier gas (He) was maintained at 0.69 × 10⁵ Pa
259 until the end of the temperature program and then ramped from 0.69 × 10⁵ Pa to 1.49 × 10⁵ Pa
260 at 0.04 × 10⁵ Pa min⁻¹. The following mass spectrometer conditions were used: electron energy
261 70 eV, source temperature 230°C, quadrupole 1 temperature 150°C, quadrupole 2 temperature
262 150°C, collision gas (N₂) flow 1.5 mL min⁻¹, quench gas (He) flow 2.25 mL min⁻¹, mass range
263 50–700 Dalton, cycle time 313 ms. DMDS derivatives were quantified in multiple reaction
264 monitoring (MRM) mode. Precursor ions were selected from the most intense ions (and specific
265 fragmentations) observed in electron ionization (EI) mass spectra. *Trans/cis* ratios were
266 obtained directly from peak area measurement of *threo* and *erythro* DMDS adducts after
267 analyses, which were carried out three times.

268

269 2.2.8. Gas chromatography-EI quadrupole time-of-flight mass spectrometry

270 Accurate mass measurements were made in full scan mode using an Agilent 7890B/7200
271 GC/QTOF system (Agilent Technologies, Parc Technopolis – ZA Courtaboeuf, Les Ulis,
272 France). A cross-linked 5% phenyl-methylpolysiloxane (Macherey-Nagel; OPTIMA-5MS
273 Accent, 30 m × 0.25 mm, 0.25 µm film thickness) capillary column was used. Analyses were
274 performed with an injector operating in pulsed splitless mode set at 270°C. Oven temperature
275 was ramped from 70°C to 130°C at 20°C min⁻¹ and then to 300°C at 5°C min⁻¹. The pressure
276 of the carrier gas (He) was maintained at 0.69 × 10⁵ Pa until the end of the temperature program.
277 Instrument temperatures were 300°C for transfer line and 230°C for the ion source. Nitrogen
278 (1.5 mL min⁻¹) was used as collision gas. Accurate mass spectra were recorded across the range
279 *m/z* 50–700 at 4 GHz with the collision gas opened. The QTOF-MS instrument provided a
280 typical resolution ranging from 8009 to 12252 from *m/z* 68.9955 to 501.9706.

281 Perfluorotributylamine (PFTBA) was used for daily MS calibration. Compounds were
282 identified by comparing their TOF mass spectra, accurate masses and retention times with those
283 of standards. Quantification of each compound involved extraction of specific accurate
284 fragment ions, peak integration and determination of individual response factors using external
285 standards.

286

287 2.2.9. Statistical analysis

288 The collected data were analyzed using the XLStat version 22.05 software (Adinsoft™).
289 Kruskal-Wallis tests associated with a pairwise multiple comparison (using the Conover-Iman
290 procedure) were performed on *trans/cis* ratios and on bacterial mortality data, at significance
291 level $\alpha = 5\%$.

292

293 3. Results

294 Chlorophyll *a* concentration in the bottommost layer of ice (0–3 cm) was 0.44, 3.93 and
295 11.76 $\mu\text{g L}^{-1}$ at St 403, St 409 and St 413, respectively. Chlorophyll *a*, phaeopigments and
296 particulate organic carbon (POC) concentrations, bacterial abundance (BA) and bacterial
297 production (BP) were measured in the upper 100 m of the water column at each station. Though
298 relatively weak along the whole transect, pelagic chlorophyll *a* concentrations were found to be
299 highest (up to 0.58 $\mu\text{g L}^{-1}$) in the upper 30 m of St 409, St 413 and St 418 (Fig. 2A). The highest
300 phaeopigment concentrations (up to 0.50 $\mu\text{g L}^{-1}$) were observed between 20 m and 40 m at
301 St 413 (Fig. 2B). The highest POC concentrations were measured in the topmost waters of St
302 409, St 413 and St 418 (values reaching 200 mg L^{-1} at the surface of St 418 and at 15 m in the
303 case of St 413) (Fig. 2C). BA was found to be relatively low at St 403 and St 409, but increased
304 from St 413 to St 418, reaching 1.9×10^6 cells mL^{-1} in the upper 30 m of water of St 418 (Fig.

305 3A). The highest values of BP (up to $0.33 \mu\text{C L}^{-1} \text{d}^{-1}$) were observed at the surface of St 409
306 and at 10 m for St 413 (Fig. 3B).

307 To learn more about the nature of the organisms present in the different ice and SPM
308 samples, the relative proportions of the main monounsaturated fatty acids (MUFAs) ($\text{C}_{16:1\Delta 9}$,
309 $\text{C}_{16:1\Delta 11}$, $\text{C}_{18:1\Delta 9}$, $\text{C}_{18:1\Delta 11}$, $\text{C}_{20:1\Delta 11}$ and $\text{C}_{22:1\Delta 11}$), and alcohols ($\text{C}_{20:1\Delta 11}$ and $\text{C}_{22:1\Delta 11}$) were
310 measured (Fig. 4). All the ice samples collected at St 403, St 409 and St 413 were dominated
311 by $\text{C}_{16:1\Delta 9}$ (palmitoleic) acid. By contrast, $\text{C}_{18:1\Delta 9}$ (oleic) acid appeared to be the dominant
312 MUFA of most of the SPM samples, except for those collected in the upper 30 m at St. 413 and
313 at the surface and between 25 m and 30 m at St 418 containing a high abundance of $\text{C}_{20:1\Delta 11}$ and
314 $\text{C}_{22:1\Delta 11}$ acids and alcohols (Fig. 4).

315 The main algal sterols – cholest-5,24-dien-3 β -ol (desmosterol), 24-methylcholesta-5,22 E -
316 dien-3 β -ol (brassicasterol), 24-methylcholesta-5,24(28)-dien-3 β -ol (24-methylenecholesterol),
317 and 24-ethylcholest-5-en-3 β -ol (sitosterol) – were quantified in ice and water samples at the
318 different stations to confirm the nature of the material present in SPM. Cholesterol, a
319 contaminant often introduced in the samples during their withdrawal and treatment, was
320 excluded from this comparison. Sea ice was found to be dominated by brassicasterol and 24-
321 methylenecholesterol at St 403 and by 24-methylenecholesterol at St 409 and St 413 (Fig. 5).
322 The deeper SPM samples collected at St 403 showed a dominance of desmosterol, while most
323 of those collected at St 409 and at St 413 were dominated by brassicasterol. Relatively high
324 proportions of desmosterol were also observed in the surface and 20 m samples of St 413 and
325 in the surface and 30 m samples of St 418 (Fig. 5).

326 To estimate the stress state of bacteria induced by salinity in brine channels of ice, *trans/cis*
327 ratios of $\text{C}_{16:1\Delta 11}$ (hexadec-11-enoic), oleic and $\text{C}_{18:1\Delta 11}$ (vaccenic) acids were measured in all the
328 samples (Fig. 6). The results obtained showed a very strong isomerization of hexadec-11-enoic
329 (*trans/cis* ratios reaching 2.1), and vaccenic (*trans/cis* ratios reaching 0.95) acids, but not of

330 oleic acid in the deeper SPM samples of St 403 and St 409 (Fig. 7). A strong isomerization of
331 hexadec-11-enoic (*trans/cis* ratio 0.8 and 0.78) and vaccenic acids (*trans/cis* ratios 0.31 and
332 0.18) was also observed in the 0–3 cm layer of ice at St 409 and St 413, respectively. At St 418,
333 the three fatty acids were strongly isomerized in the upper SPM samples (*trans/cis* ratio
334 reaching 0.6, 1.0 and 0.45 for hexadec-11-enoic, oleic and vaccenic acids, respectively) (Fig. 7).

335 The viability of bacteria was estimated with PMA in sea ice and SPM samples collected at
336 St 409 and in SPM samples collected at St 418. At St 409, a high bacterial mortality was
337 observed in sea ice (88.7 and 84.3% in the 3–10 and 0–3 cm layers, respectively) and in the
338 10 m SPM sample (62.3%), but not in the 20 m sample (Table 1). In the deeper (≥ 30 m) SPM
339 samples collected at St 418, bacterial mortality was found to be very low, but it was relatively
340 high in the surface and 20 m samples (23.3 and 67.5%, respectively) (Table 1).

341

342 **4. Discussion**

343

344 *4.1. Composition of sea ice and SPM samples*

345 The low chlorophyll *a* concentrations measured in the bottommost ice samples
346 corresponded to only one-tenth of the values previously observed at the time of the sympagic
347 algal bloom at the GreenEdge ice camp located near Broughton Island in Baffin Bay (Fig. 1)
348 (Amiriaux et al., 2019). It thus seems that the bloom of sympagic algae took place before the
349 start of sampling. The increase in chlorophyll *a* concentration observed in this layer from St 403
350 to St 413 was thus attributed to the growth of the epiphytic diatom *Melosira arctica*, whose
351 presence was noted during the sampling (Amiriaux, unpublished data). The fatty acid profiles
352 of all the sea ice samples were dominated by C_{16:1Δ9} (palmitoleic) acid (Fig. 4) well-known to
353 be the main fatty acid component of sea ice-associated (sympagic or epiphytic) diatoms (Fahl
354 and Kattner, 1993; Falk-Petersen et al., 1998; Leu et al., 2010). The algal community present

355 in the 0–3 cm sample at St 403 seemed to be mainly composed of pennate and centric
356 (*M. arctica*?) diatoms and Thalassiosirales as suggested by the dominance of brassicasterol and
357 24-methylenecholesterol (Rampen et al., 2010) (Fig. 5). The increasing proportions of 24-
358 methylenecholesterol observed at St 409 and St 413 were attributed to the presence of
359 increasing amounts of *M. arctica* (containing a significant proportion of this sterol, Smik,
360 unpublished data).

361 It is well known that sea ice retreat controls the timing of summer plankton blooms in the
362 Arctic Ocean (Janout et al., 2016). From visual observation and knowledge of bloom dynamics,
363 a chlorophyll *a* threshold of $0.5 \mu\text{g L}^{-1}$ was defined by Perrette et al. (2011) to identify the
364 blooms in the Arctic. The chlorophyll *a* concentrations measured in the water column along the
365 transect investigated (up to $0.58 \mu\text{g L}^{-1}$) only exceeded this threshold between 0 and 20 m at St
366 409 and between 15 m and 35 m at St 413 (Fig. 2A), suggesting the presence of a weak ice-
367 edge bloom at these stations. In the ice-covered water column, chlorophyll may result from: (i)
368 the growth of pelagic phytoplankton or (ii) the release of non-aggregated sympagic or epiphytic
369 algae during melting. The former hypothesis is well supported by the dominance of
370 brassicasterol observed in surface SPM samples (brassicasterol/24-methylenecholesterol ratio
371 1.0–1.8) (Fig. 5), which contrasts with the dominance of 24-methylenecholesterol in the
372 bottommost layer of sea ice at these stations (brassicasterol/24-methylenecholesterol ratio 0.07–
373 0.7) (Fig. 5). This dominance of brassicasterol probably results from the presence of the
374 prymnesiophyte *Phaeocystis pouchetii*, whose sterol fraction is known to consist of almost
375 100% brassicasterol (Nichols et al., 1991) and which is a main component of under-ice and
376 spring blooms across the Arctic (Riisgaard et al., 2015). Microscopic examination of some SPM
377 samples supported this explanation (e.g. percentage of *Phaeocystis* to protists at 30 m at St 413
378 $\approx 50\%$) (Babin, unpublished data). However, during sea ice melting the species composition of
379 dispersed and aggregated algae may differ significantly (Riebesell et al., 1991). Proportionately

380 more cells of weakly aggregated pennate diatoms containing high proportions of brassicasterol
381 (Rampen et al., 2010) may thus stay suspended, while other more aggregated ice algae (e.g.
382 Thalassiosirales or *M. arctica*) incorporated into sinking particles should rapidly sink out of the
383 euphotic zone (Riebesell et al., 1991).

384 A high zooplanktonic grazing activity, well supported by the high abundance of C_{20:1Δ11}
385 and C_{22:1Δ11} alkan-1-ols, was observed in the upper 30 m at St 413 and at the surface and between
386 25 m and 30 m at St 418 (Fig. 4). Wax esters are generally the main storage lipids of marine
387 zooplankton in high-latitude species (Lee et al., 2006) and the most common alkan-1-ols of the
388 wax esters found in herbivorous zooplankton are C_{20:1Δ11} and C_{22:1Δ11} alkan-1-ols (Lee and
389 Nevenzel, 1979; Albers et al., 1996). These alcohols are only known to occur in copepods that
390 undergo diapause (Graeve et al., 1994), which are widely distributed in the Arctic.

391 In this area, dominant herbivorous zooplankton are the three large *Calanus hyperboreus*,
392 *C. glacialis* and *C. finmarchicus* in addition to the smallest *Pseudocalanus spp.* (Sameoto,
393 1984; Forest et al., 2012). At this period of the year, naupliis and copepodits depend on the
394 bloom to develop into adults, and diapausing adults metabolize primary production into highly
395 rich esters stocks (Conover and Huntley, 1991; Falk-Petersen et al., 2009). A study on the
396 surface copepod community of Baffin Bay from Underwater Vision Profiler (UVP) data
397 revealed that a lot a small copepods were actively feeding in the eastern and ice-free waters
398 (including St 418) during the GreenEdge cruise (Vilgrain et al., submitted). Complementary
399 data from net sampling showed that ice-free stations are dominated by young stages of *C.*
400 *finmarchicus* and *C. glacialis* (naupliis, and stages CI to CVI) in addition with CII to CIV stages
401 of *C. hyperboreus* (Fig. S1). All stages of *Pseudocalanus spp.* were also more abundant in St
402 413 and 418 with naupliis in particular (Fig. S1). The large proportion of young herbivorous
403 stages was expected in ice-free stations according to their life cycle strategies (Hirche and
404 Niehoff 1996; Soreide et al., 2010). Adults of all these species were generally distributed all

405 over the Bay, but diapausing species such as *Calanus spp.*, are probably metabolizing esters
406 from phytoplanktonic precursors, which could explain the presence of C_{20:1Δ11} and C_{22:1Δ11}
407 alkan-1-ols at St 413 and St 418.

408 Although the degradation of chlorophyll *a* to phaeopigments occurs in the guts of both
409 large and small macro-zooplankton (Nelson, 1989), these compounds could be detected in
410 significant proportions only at 30 m at St 413 (Fig. 2B). The low concentrations of
411 phaeopigments observed in the upper SPM samples of St 413 may be attributed to
412 photooxidation processes, well known to degrade such pigments quickly (Welschmeyer and
413 Lorenzen, 1985) and strongly favored at St 413 due to the lack of snow cover and the relatively
414 thin ice (limited to 40 cm). Despite the very high copepod activity present at 30 m at St 418
415 (Fig. 5), phaeopigment concentration was found to be very weak (Fig. 2B), probably owing to
416 a particularly intense photooxidation at this open water station. As expected, in the samples
417 where the presence of high proportions of copepods was indicated by C_{20:1Δ11} and C_{22:1Δ11} alkan-
418 1-ols, large proportions of their two main sterols (Harvey et al., 1987) cholesterol (not shown)
419 and desmosterol (Fig. 5) could be observed.

420 The deepest SPM samples collected at St 403 were characterized by (i) very low
421 chlorophyll *a* concentrations (Fig. 2A), (ii) high proportions of oleic acid (Fig. 4) and
422 desmosterol (Fig. 5) and (iii) lack of C_{20:1Δ11} and C_{22:1Δ11} alkan-1-ols. Oleic acid is often
423 enriched in secondary producers (Falk-Petersen et al., 1999) and thus commonly interpreted as
424 a marker of heterotrophic feeding (Graeve et al., 1997; Tolosa et al., 2004). Moreover,
425 desmosterol is produced by zooplankton during the conversion of dietary phytosterols to
426 cholesterol (Harvey et al., 1987). Given the absence of alkanols, the presence of copepods in
427 these samples was excluded and that of micro-zooplankton suspected. In Baffin Bay, it is well
428 known that the ice microfauna is dominated by dinoflagellates and ciliates (Michel et al., 2002),
429 rarely observed in the water column, probably because prey are too scarce. These SPM samples

430 thus seem to contain herbivorous micro-zooplankton feeding in ice and then released in the
431 water column during melting. The presence of *trans* MUFAs, typical of stressed sympagic
432 bacteria (see 4.2.), suggests the simultaneous presence of sympagic herbivorous and
433 bacterivorous micro-zooplankton in these samples. In the deepest samples of St 409
434 characterized by very low amounts of sterols (Fig. 5), only bacterivorous micro-zooplankton,
435 generally incapable of synthesizing or incorporating sterols (Breteler et al., 2004), seem present.

436 SPM material collected between 10 m and 20 m of the open water station St 418 exhibited
437 relatively high proportions of hexadec-11-enoic and vaccenic acids (Fig. 4), well known to be
438 specific to bacteria (Lambert and Moss, 1983; Sicre et al., 1988). Most of the oleic acid present
439 in these samples also arises from bacteria (see Section 4.2.). These samples thus contained a
440 large proportion of bacteria (Fig. 4). These observations are consistent with the highest BA
441 measured in these samples (Fig. 3A), which is similar to those previously measured in spring
442 in sea ice of the Chukchi Sea ($0.7\text{--}2.5 \times 10^6$ cells mL⁻¹; Meiners et al., 2008). Arctic sea ice
443 harbors large amounts of extracellular polymeric substances (EPS) in both the dissolved and
444 particulate fractions (Krembs and Engel, 2001; Krembs et al., 2002; Meiners et al., 2003). Some
445 authors (Riedel et al., 2006; Juhl et al., 2011) previously demonstrated that EPS retained within
446 the melting sea ice in the Arctic could supply a pulse of organic carbon to surface waters after
447 most of the sea-ice algal biomass has been released into the water column. In the pelagic realm,
448 EPS-rich particles, which have been observed to be positively or neutrally buoyant (Azetsu-
449 Scott and Passow, 2004; Meiners et al., 2008), are densely colonized by attached bacteria and
450 are ideal vectors for their horizontal distribution (Meiners et al., 2008). Bacteria use these
451 particles as sites of attachment, possibly to protect them from grazers (Salcher et al., 2005), or
452 as a carbon-rich substrate, which could enhance bacterial production (Riedel et al., 2006). These
453 exopolymers could thus ascend in association with attached bacteria (Azetsu-Scott and Passow,
454 2004). The highest abundances of bacteria observed at 10 m and 20 m at St 418 (Fig. 3A) were

455 thus attributed to the release of EPS particles heavily colonized by bacteria during sea ice
456 melting after previous loss of the sympagic algal biomass.

457

458 4.2. Stress state of bacteria in sea ice and SPM particles

459 *Cis-trans* isomerization of MUFAs has been shown to serve as an adaptive response to
460 chemical or osmotic stress in strains of the widespread genera *Pseudomonas* and *Vibrio*
461 (Okuyama et al., 1991; Heipieper et al., 1992; Molina- Santiago et al., 2017). High *trans/cis*
462 vaccenic acid ratios were previously observed in sinking particles collected during the 2015
463 and 2016 GreenEdge ice camps (Amiriaux et al., 2017; Amiriaux et al., 2021a). These high
464 values were attributed to release of non-growing bacteria attached to sympagic algae stressed
465 by salinity in internal brine channels during the early stages of sea ice melting. To determine
466 whether bacteria attached to suspended particles were also stressed by salinity, *trans/cis* ratios
467 of the main monounsaturated fatty acids present in *Pseudomonas sp.* and *Vibrio sp.* (hexadec-
468 11-enoic, oleic and vaccenic acids) (Lambert et al., 1983; Holsmtröm et al., 1998; Jia et al.,
469 2014) were measured in sea ice and in SPM samples along the transect investigated. Although
470 present in some *Vibrio sp.* (Lambert et al., 1983; Jia et al., 2014), palmitoleic acid was excluded
471 from these measurements owing to its lack of specificity (strong dominance in sympagic and
472 pelagic diatoms) (Fahl and Kattner, 1993; Leu et al., 2010).

473 Very high *trans/cis* ratios of hexadec-11-enoic and vaccenic acids were observed in the
474 deepest SPM samples of St 403 and St 409 (Fig. 7), which seemed to be dominated by micro-
475 zooplankton (see Section 4.1.). It was previously observed that the lipid composition (fatty acids
476 and neutral lipids) of bacterivorous ciliates resembled that of their prey (Harvey et al., 1987;
477 Boëchat and Adrian, 2005). The high *trans/cis* values observed in these samples were thus
478 attributed to (i) the ingestion of bacteria stressed by salinity in internal brines of sea ice by
479 sympagic ciliates, (ii) the direct incorporation of highly isomerized dietary fatty acids and

480 (iii) the release of these bacterivorous ciliates in the water column during ice melting. The well-
481 known biosynthesis of *cis*-oleic acid during the metabolism of ciliates (Erwin and Bloch, 1963)
482 is consistent with the relatively weak *trans/cis* ratio of this acid observed in these SPM samples
483 (Fig. 7). Brine salinity, which could not be measured during the cruise, are expected to be low
484 at the time of sampling (summer). However, high brine salinity values (ranging from 50 to 70)
485 were measured in May 2015 and 2016 in the upper part of the ice at Qikiqtarjuaq (GreenEdge
486 fixed station relatively close to the transect investigated, Fig. 1) (Amiriaux et al., 2019; 2021a).
487 Non-halophilic bacteria strongly affected by these hypersaline conditions in spring could thus
488 have been ingested by sympagic ciliates and trapped in the ice before to be released in the water
489 column during the summer melting period.

490 It is well known that the uppermost section of the ice experiences the most drastic changes
491 in brine salinity (Ewert and Deming, 2013). As a consequence, bacteria attached to sympagic
492 algae in the bottommost ice are generally not highly affected by osmotic stress (Rontani et al.,
493 2018; Amiriaux et al., 2021a). The high *trans/cis* ratios of hexadec-11-enoic and vaccenic acids
494 measured in the bottommost 3 cm of ice of St 409 and St 413 (Figs. 6 and 7) were thus
495 surprising. Given the relative similarity of these ratios with those observed in the deepest
496 samples of St 403 and St 409 (Fig. 7), this isomerization was attributed to the presence of ciliates
497 fed on salinity-stressed bacteria in internal brine channels and trapped during their discharge at
498 the bottom of ice.

499 It is generally considered that suspended particles, which constitute most of the standing
500 stock of particulate matter in the ocean (Wakeham and Lee, 1989), sink very slowly through
501 the water column. However, aggregation processes, the extent of which remains to be estimated
502 (Wakeham and Lee 1989; Hill 1998), can strongly increase the settling velocity of these
503 particles and thus their contribution to the seafloor. Sympagic microzooplankton can thus

504 contribute to the transfer of the signature of bacteria stressed by hypersaline conditions in brine
505 channels of sea ice to the sediments.

506 SPM material collected in the topmost waters of St 418 seems to be composed of EPS
507 particles retained in sea ice and discharged in seawater after the initial release of algal biomass
508 (Riedel et al., 2006; Juhl et al., 2011). Such EPS particles contain high amounts of bacteria
509 (Meiners et al., 2008) that may be of sympagic or pelagic origin. The very high *trans/cis* ratios
510 of hexadec-11-enoic, vaccenic and oleic acids observed in these SPM samples (Fig. 7)
511 demonstrate that the bacteria attached to EPS particles are strongly stressed by salinity and thus
512 arise from sea ice. The strong isomerization of oleic acid observed also attests to the bacterial
513 origin of this acid. In the presence of osmotic stress, CTI activity is used by bacteria as an urgent
514 response to guarantee survival, before other adaptive mechanisms (Heipieper et al., 2007).
515 Consequently, with no osmotic stress (as is the case in the water column) the *trans/cis* ratio of
516 bacteria stressed by salinity in brine channels of sea ice should decrease to the basic level
517 (Fischer et al., 2010). Since conversion of *trans* to *cis* fatty acids is not catalyzed (Eberlein et
518 al., 2018), recovery of the regularly low *trans/cis* ratio needs *de novo* synthesis of *cis* fatty acids
519 and thus depends on bacterial growth rates. The very high values of the *trans/cis* ratio observed
520 in the topmost waters of St 418 (Fig. 7) are thus indicative of the non-growing state of bacteria
521 attached to EPS particles. This assumption is well supported by the relatively weak BP
522 measured in these samples (Fig. 3B) exhibiting the highest BA (Fig. 3A).

523

524 4.3. Viability of attached bacteria in sea ice and SPM particles

525 PMA treatment showed that most of the bacteria associated with sympagic algae at St 409
526 had disrupted membranes and so were dead (Table 1). These results are consistent with the high
527 mortality of attached bacteria measured in sea ice at the end of the 2016 GreenEdge ice camp
528 (Amiriaux et al., 2021a) and attributed to the bactericidal properties of free fatty acids (FFAs)

529 released by sympagic algae under the effect of light stress. The toxicity of FFAs results from
530 their insertion into the bacterial inner membrane, increasing its permeability and letting internal
531 contents leak from the cell, which can result in death (Boyaval et al., 1995; Shin et al., 2007).
532 A high mortality was also observed in the 10 m SPM sample (Table 1). This suggests that the
533 algal material present in this sample (Fig. 5) results from the release of non-aggregated and
534 FFA-producing sympagic diatoms during ice melting rather than from the growth of pelagic
535 algae. By contrast, the viability of bacteria attached to suspended particles collected at 20 m
536 and dominated by micro-zooplankton was found to be very good (Table 1).

537 Concerning SPM samples collected at St 418, PMA revealed a very low mortality of
538 attached bacteria in the deeper (≥ 30 m) samples (Table 1). This good viability is probably due
539 to the presence of unstressed bacteria associated with copepod or micro-zooplankton material,
540 which dominated these samples (see Section 4.1.). By contrast, a lower viability was observed
541 in the samples collected at the surface and at 20 m (23.3 and 67.5% of mortality, respectively)
542 (Table 1). The 20 m sample mainly composed of EPS particles thus contained a mixture of dead
543 bacteria (in which the integrity of cell membranes could not be maintained) and non-growing
544 bacteria (where *cis-trans* isomerization of monounsaturated fatty acids ensured membrane
545 stiffness but not growth). The presence of a significant proportion of zooplanktonic material
546 (potential supports of unstressed bacteria) in the surface sample (Fig. 4) could explain the lower
547 mortality (relative to the 20 m sample) observed (Table 1).

548

549 *4.4. Considerations about the preservation and transfer of sympagic material to the seafloor*

550 The preservation of sympagic algae during their transfer in the water column depends
551 mostly on grazing by zooplankton and mineralization by their attached bacteria. We previously
552 demonstrated that during the early stages of ice melting, bacteria associated to sinking sympagic
553 material have been strongly stressed in hypersaline brine channels and are thus mainly non-

554 growing in these particles (Amiriaux et al., 2017). In contrast, during the advances stages of
555 melting most bacteria associated to sinking ice algae appeared to be stressed by free fatty acids
556 and dead (Amiriaux et al., 2021a).

557 Whereas only a small part of the sympagic material is released during the early stages
558 of ice melting, i.e. when bacteria are stressed by hypersaline conditions (Amiriaux et al., 2021a,
559 2021b), a strong *cis-trans* isomerization of MUFAs was previously observed in Arctic
560 sediments (Rontani et al., 2012; Amiriaux et al., 2017). The results obtained during the present
561 study allow to propose an explanation to this paradox. Indeed, during the early stages of ice
562 melting feeding of sympagic microzooplankton on stressed bacteria results to the incorporation
563 and transfer of that stress signal (after aggregation) to the deeper waters, whereas at the
564 advanced stages of melting copepods intensively assimilate the sympagic material (EPS-rich
565 particles and sea ice algae) released in the water column. Due to the good healthy state of
566 bacteria associated to the resulting copepod fecal pellets, this material should be degraded
567 intensively within the water column contributing only weakly to the sediments. It thus appears
568 that trophic relationships between sea-ice algae, their associated bacteria and zooplanktonic
569 grazers are strongly intricate and need to be more investigated.

570

571 **5. Conclusions**

572 Lipid analyses and propidium monoazide (PMA) method allowed the monitoring of the
573 stress and viability of attached bacteria in sea ice and SPM samples collected during the
574 GreenEdge 2016 cruise in Baffin Bay, along a transect from sea ice to open water. Our results
575 are summarized in a conceptual trophic network scheme (Fig. 8).

576 At the western stations ice covered St 403 and St 409 lipid analyses showed a strong *cis-*
577 *trans* isomerization of MUFAs attributed to the presence of sympagic bacterivorous
578 microzooplankton (ciliates) incorporating *trans* fatty acids after ingestion of bacteria

579 osmotically stressed in hypersaline brine channels of ice (Fig. 8). At the St 409, the high
580 bacterial mortality measured in sea ice is consistent with that previously observed during the
581 GreenEdge 2016 ice camp (Amiriaux *et al.*, 2021a) and is likely due to the release of bactericidal
582 FFAs by sympagic algae under the effect of light stress (Fig. 8).

583 At the eastern ice-covered station St 413 and open water station St 418 the lipid analysis
584 showed a high proportion of macro-zooplankton (copepods) (Fig. 8). SPM material collected
585 in shallower waters at the open water St 418 seems to be mainly composed of EPS-rich particles
586 retained in sea ice and discharged in seawater after the initial release of algal biomass. In those
587 waters, most of the bacteria associated to this material appeared to be either dead or in a non-
588 growing state, while these attached to deeper SPM of St 418 (dominated by zooplanktonic
589 material) were in good healthy state (Fig. 8).

590 2021a2021b

591 **Acknowledgments**

592 This work was supported by the Bacstress (INSU-EC2CO-Microbien) and GreenEdge
593 projects. The GreenEdge project is funded by the following French and Canadian programs and
594 agencies: ANR (Contract #111112), CNES (project #131425), IPEV (project #1164), CSA,
595 Fondation Total, ArcticNet, LEFE and the French Arctic Initiative (GreenEdge project). This
596 project was made possible by the support of the Hamlet of Qikiqtarjuaq and the members of the
597 community and of the Inuksuit School and its Principal Jacqueline Arsenault. The project is
598 conducted under the scientific coordination of the Canada Excellence Research Chair on
599 Remote sensing of Canada's new Arctic frontier and the CNRS & Université Laval Takuvik
600 Joint International laboratory (UMI3376). The field campaign owed its success to the
601 contributions of J. Ferland, G. Bécu, C. Marec, J. Lagunas, F. Bruyant, J. Larivière, E. Rehm,
602 S. Lambert-Girard, C. Aubry, C. Lalande, A. LeBaron, C. Marty, J. Sansoulet, D. Christiansen-
603 Stowe, A. Wells, M. Benoît-Gagné, E. Devred and M.-H. Forget from the Takuvik laboratory,

604 C.J. Mundy from the University of Manitoba and F. Pinczon du Sel and E. Brossier from
605 Vagabond. We also thank Québec-Océan, the CCGS *Amundsen* and the Polar Continental Shelf
606 Program for their in-kind contribution in polar logistics and scientific equipment. Thanks are
607 also due to the Feder Oceanomed (No. 1166-39417) for the funding of the GC-QTOF and GC-
608 MS/MS employed. We are also grateful to three anonymous reviewers for their useful and
609 constructive comments.

610

611 **References**

- 612 Albers CS, Kattner G, Hagen W. The compositions of wax esters, triacylglycerols and
613 phospholipids in Arctic and Antarctic copepods: evidence of energetic adaptations. *Mar*
614 *Chem* 1996;**55**:347–58.
- 615 Amiraux R, Belt ST, Vaultier F *et al.* Monitoring photo-oxidative and salinity-induced bacterial
616 stress in the Canadian Arctic using specific lipid tracers. *Mar Chem* 2017;**194**:89–99.
- 617 Amiraux R, Burot C, Bonin P *et al.* Stress factors resulting from the Arctic vernal sea ice melt:
618 impact on the viability of the bacterial communities associated to sympagic algae. *Elem*
619 *Sci Anth* 2021a. (*In press*)
- 620 Amiraux R, Rontani J-F, Armougom F *et al.* Bacterial diversity and lipid biomarkers in sea ice
621 and sinking particulate organic material during the melt season in the Canadian Arctic.
622 *Elem Sci Anth* 2021b. (*In press*)
- 623 Amiraux R, Smik L, Köseoğlu D *et al.* Temporal evolution of IP₂₅ and other highly branched
624 isoprenoid lipids in sea ice and the underlying water column during an Arctic melting
625 season. *Elem Sci Anth* 2019;**7**:38.
- 626 Azetsu-Scott K, Passow U. Ascending marine particles: Significance of transparent exopolymer
627 particles (TEP) in the upper ocean. *Limnol Oceanogr* 2004;**49**:741–8.

628 Barrett SM, Volkman JK, Dunstan GA *et al.* Sterols of 14 Species of Marine Diatoms
629 (Bacillariophyta). *J Phycol* 1995;**31**:360–9.

630 Bates SS, Cota GF. Fluorescence Induction and Photosynthetic Responses of Arctic Ice Algae
631 to Sample Treatment and Salinity. *J Phycol* 1986;**22**:421–9.

632 Bidle KD, Azam F. Accelerated dissolution of diatom silica by marine bacterial assemblages.
633 *Nature* 1999;**397**:508–12.

634 Boëchat IG, Adrian R. Biochemical composition of algivorous freshwater ciliates: You are not
635 what you eat. *FEMS Microbiol Ecol* 2005;**53**:393–400.

636 Boetius A, Albrecht S, Bakker K *et al.* Export of Algal Biomass from the Melting Arctic Sea
637 Ice. *Science* 2013;**339**:1430–2.

638 Boetius A, Anesio AM, Deming JW *et al.* Microbial ecology of the cryosphere: sea ice and
639 glacial habitats. *Nat Rev Microbiol* 2015;**13**:677–90.

640 Boras JA, Sala MM, Arrieta JM *et al.* Effect of ice melting on bacterial carbon fluxes channeled
641 by viruses and protists in the Arctic Ocean. *Polar Biol* 2010;**33**:1695–707.

642 Boyaval P, Corre C, Dupuis C *et al.* Effects of free fatty acids on propionic acid bacteria. *Lait*
643 1995;**75**:17–29.

644 Breteler W, Koski M, Rampen S. Role of essential lipids in copepod nutrition: no evidence for
645 trophic upgrading of food quality by a marine ciliate. *Mar Ecol Prog Ser* 2004;**274**:199–
646 208.

647 Buser HRudolf, Arn Heinrich, Guerin Patrick *et al.* Determination of double bond position in
648 mono-unsaturated acetates by mass spectrometry of dimethyl disulfide adducts. *Anal*
649 *Chem* 1983;**55**:818–22.

650 Cho BC, Azam F. Major role of bacteria in biogeochemical fluxes in the ocean's interior.
651 *Nature* 1988;**332**:441–3.

652 Conover RJ, Huntley M. Copepods in ice-covered seas—Distribution, adaptations to seasonally
653 limited food, metabolism, growth patterns and life cycle strategies in polar seas. *J Mar*
654 *Syst* 1991;**2**:1–41.

655 Cooksey K, Wigglesworth-Cooksey B. Adhesion of bacteria and diatoms to surfaces in the sea:
656 a review. *Aquat Microb Ecol* 1995;**9**:87–96.

657 Ducklow H. Bacterial Production and Biomass in the Oceans. *Microbial Ecology of the Oceans*.
658 Vol 1. Wiley & Sons, 2000, 85–120.

659 Dupont F. Impact of sea-ice biology on overall primary production in a biophysical model of
660 the pan-Arctic Ocean. *J Geophys Res Oceans* 2012;**117**, DOI: [10.1029/2011JC006983](https://doi.org/10.1029/2011JC006983).

661 Eberlein C, Baumgarten T, Starke S *et al.* Immediate response mechanisms of Gram-negative
662 solvent-tolerant bacteria to cope with environmental stress: *cis-trans* isomerization of
663 unsaturated fatty acids and outer membrane vesicle secretion. *Appl Microbiol Biotechnol*
664 2018;**102**:2583–93.

665 Engel A, Passow U. Carbon and nitrogen content of transparent exopolymer particles (TEP) in
666 relation to their Alcian Blue adsorption. *Mar Ecol Prog Ser* 2001;**219**:1–10.

667 Erwin J, Bloch K. Lipid metabolism of ciliated protozoa. *J Biol Chem* 1963;**238**:1618–24.

668 Ewert M, Deming J. Sea ice microorganisms: environmental constraints and extracellular
669 responses. *Biology* 2013;**2**:603–28.

670 Fahl K, Kattner G. Lipid Content and fatty acid composition of algal communities in sea-ice
671 and water from the Weddell Sea (Antarctica). *Polar Biol* 1993;**13**:405–9.

672 Falk-Petersen S, Mayzaud P, Kattner G *et al.* Lipids and life strategy of Arctic *Calanus*. *Mar*
673 *Biol Res* 2009;**5**:18–39.

674 Falk-Petersen S, Sargent JR, Henderson J *et al.* Lipids and fatty acids in ice algae and
675 phytoplankton from the Marginal Ice Zone in the Barents Sea. *Polar Biol* 1998;**20**:41–7.

676 Falk-Petersen S, Sargent JR, Lønne OJ *et al.* Functional biodiversity of lipids in Antarctic
677 zooplankton: *Calanoides acutus*, *Calanus propinquus*, *Thysanoessa macrura* and
678 *Euphausia crystallorophias*. *Polar Biol* 1999;**21**:37–47.

679 Fernandes SO, Javanaud C, Michotey VD *et al.* Coupling of bacterial nitrification with
680 denitrification and anammox supports N removal in intertidal sediments (Arcachon Bay,
681 France). *Estuar Coast Shelf Sci* 2016;**179**:39–50.

682 Fernández-Méndez M, Katlein C, Rabe B *et al.* Photosynthetic production in the central Arctic
683 Ocean during the record sea-ice minimum in 2012. *Biogeosciences* 2015;**12**:3525–49.

684 Fischer J, Schauer F, Heipieper HJ. The *trans/cis* ratio of unsaturated fatty acids is not
685 applicable as biomarker for environmental stress in case of long-term contaminated
686 habitats. *Appl Microbiol Biotechnol* 2010;**87**:365–71.

687 Forest A, Stemmann L, Picheral M *et al.* Size distribution of particles and zooplankton across
688 the shelf-basin system in southeast Beaufort Sea: combined results from an Underwater
689 Vision Profiler and vertical net tows. *Biogeosciences* 2012;**9**:1301–20.

690 Forest A, Tremblay J-É, Gratton Y *et al.* Biogenic carbon flows through the planktonic food
691 web of the Amundsen Gulf (Arctic Ocean): A synthesis of field measurements and inverse
692 modeling analyses. *Prog Oceanogr* 2011;**91**:410–36.

693 Garrison DL, Buck KR. Organism losses during ice melting: A serious bias in sea ice
694 community studies. *Polar Biol* 1986;**6**:237–9.

695 Ghiglione JF, Mevel G, Pujo-Pay M *et al.* Diel and seasonal variations in abundance, activity,
696 and community structure of particle-attached and free-living bacteria in NW
697 Mediterranean Sea. *Microb Ecol* 2007;**54**:217–31.

698 Glud RN, Rysgaard S. *Carbon Cycling in Arctic Marine Ecosystems: Case Study Young Sound*.
699 Museum Tusulanum Press., 2007.

700 Gosselin M, Legendre L, Therriault J-C *et al.* Physical control of the horizontal patchiness of
701 sea-ice microalgae. *Mar Ecol Prog Ser* 1986;**29**:289–98.

702 Graeve M, Kattner G, Hagen W. Diet-induced changes in the fatty acid composition of Arctic
703 herbivorous copepods: Experimental evidence of trophic markers. *J Exp Mar Biol Ecol*
704 1994;**182**:97–110.

705 Graeve M, Kattner G, Piepenburg D. Lipids in Arctic benthos: does the fatty acid and alcohol
706 composition reflect feeding and trophic interactions? *Polar Biol* 1997;**18**:53–61.

707 Guckert JB. Phospholipid ester-linked fatty acid profile changes during nutrient deprivation of
708 *Vibrio cholerae*: Increases in the *trans/cis* Ratio and Proportions of Cyclopropyl Fatty
709 Acids. *Appl Environ Microbiol* 1986;**52**:794–801.

710 Harvey HR, Eglinton G, O’Hara SCM *et al.* Biotransformation and assimilation of dietary lipids
711 by *Calanus* feeding on a dinoflagellate. *Geochim Cosmochim Acta* 1987;**51**:3031–40.

712 Heipieper HJ, Diefenbach R, Keweloh H. Conversion of *cis* unsaturated fatty acids to *trans*, a
713 possible mechanism for the protection of phenol-degrading *Pseudomonas putida* P8 from
714 substrate toxicity. *Appl Environ Microbiol* 1992;**58**:1847–52.

715 Heipieper HJ, Meinhardt F, Segura A. The *cis–trans* isomerase of unsaturated fatty acids in
716 *Pseudomonas* and *Vibrio*: biochemistry, molecular biology and physiological function of
717 a unique stress adaptive mechanism. *FEMS Microbiol Lett* 2003;**229**:1–7.

718 Heipieper HJ, Neumann G, Cornelissen S *et al.* Solvent-tolerant bacteria for biotransformations
719 in two-phase fermentation systems. *Appl Microbiol Biotechnol* 2007;**74**:961–73.

720 Hill PS. Controls on floc size in the sea. *Oceanogr* 1998;**11**:13–18.

721 Hirche H-J, Niehoff B. Reproduction of the Arctic copepod *Calanus hyperboreus* in the
722 Greenland Sea-field and laboratory observations. *Polar Biol* 1996;**16**:209–19.

723 Holmström C, James S, Neilan BA *et al.* *Pseudoalteromonas tunicata* sp. nov., a bacterium that
724 produces antifouling agents. *Int J Syst Bacteriol* 1998;**48**:1205–12.

725 Hoppe H-G. Microbial extracellular enzyme activity: a new key parameter in aquatic ecology.
726 In: Chróst RJ (ed.). *Microbial Enzymes in Aquatic Environments*. New York, NY:
727 Springer New York, 1991, 60–83.

728 Howard-Jones MH, Ballard VD, Allen AE *et al.* Distribution of bacterial biomass and activity
729 in the marginal ice zone of the central Barents Sea during summer. *J Mar Syst*
730 2002;**38**:77–91.

731 Janout MA, Hölemann J, Waite AM *et al.* Sea-ice retreat controls timing of summer plankton
732 blooms in the Eastern Arctic Ocean. *Geophys Res Lett* 2016;**43**:12,493-12,501.

733 Jia J, Chen Y, Jiang Y *et al.* Visualized analysis of cellular fatty acid profiles of *Vibrio*
734 *parahaemolyticus* strains under cold stress. *FEMS Microbiol Lett* 2014;**357**:92–8.

735 Juhl A, Krembs C, Meiners K. Seasonal development and differential retention of ice algae and
736 other organic fractions in first-year Arctic sea ice. *Mar Ecol Prog Ser* 2011;**436**:1–16.

737 Junge K, Eicken H, Deming JW. Bacterial activity at -2 to -20°C in Arctic wintertime sea ice.
738 *Appl Environ Microbiol* 2004;**70**:550–7.

739 Karner M, Herndl GJ. Extracellular enzymatic activity and secondary production in free-living
740 and marine-snow-associated bacteria. *Mar Biol* 1992;**113**:341–7.

741 Kim LH, Chong TH. Physiological responses of salinity-stressed *Vibrio* sp. and the effect on
742 the biofilm formation on a nanofiltration membrane. *Environ Sci Technol* 2017;**51**:1249–
743 58.

744 Kirchman D, K’Nees E, Hodson R. Leucine incorporation and its potential as a measure of
745 protein synthesis by bacteria in natural aquatic systems. *Appl Environ Microbiol*
746 1985;**49**:599–607.

747 Krause-Jensen D. Benthic primary production in Young Sound, Northeast Greenland. *Medd*
748 *Grønl* 2007;**58**:159–74.

749 Krembs C, Eicken H, Junge K *et al.* High concentrations of exopolymeric substances in Arctic
750 winter sea ice: implications for the polar ocean carbon cycle and cryoprotection of
751 diatoms. *Deep Sea Res Part I Oceanogr* 2002;**49**:2163–81.

752 Krembs C, Engel A. Abundance and variability of microorganisms and transparent exopolymer
753 particles across the ice/water interface of melting first-year sea ice in the Laptev Sea
754 (Arctic). *Mar Biol* 2001;**138**:1370–7.

755 Lambert MA, Hickman-Brenner FW, Hi JJF *et al.* Differentiation of Vibvionaceae species by
756 their cellular fatty acid composition. *Int J Syst Bacteriol* 1983;**33**:777–92.

757 Lambert MA, Moss CW. Comparison of the effects of acid and base hydrolyses on hydroxy
758 and cyclopropane fatty acids in bacteria. *J Clin Microbiol* 1983;**18**:1370–7.

759 Lee R, Hagen W, Kattner G. Lipid storage in marine zooplankton. *Mar Ecol Prog Ser*
760 2006;**307**:273–306.

761 Lee RF, Nevenzel JC. Wax esters in the marine environment: origin and composition of the
762 wax from Bute Inlet, British Columbia. *J Fish Res Bd Can* 1979;**36**:1519–23.

763 Leu E, Wiktor J, Søreide J *et al.* Increased irradiance reduces food quality of sea ice algae. *Mar*
764 *Ecol Prog Ser* 2010;**411**:49–60.

765 Loffeld B, Keweloh H. *Cis-trans* isomerization of unsaturated fatty acids as possible control
766 mechanism of membrane fluidity in *Pseudomonas putida* P8. *Lipids* 1996;**31**:811–5.

767 Mancuso Nichols CA, Garon S, Bowman JP *et al.* Production of exopolysaccharides by
768 Antarctic marine bacterial isolates. *J Appl Microbiol* 2004;**96**:1057–66.

769 Mari X. Carbon content and C:N ratio of transparent exopolymeric particles (TEP) produced
770 by bubbling exudates of diatoms. *Mar Ecol Prog Ser* 1999;**183**:59–71.

771 Marie D, Partensky F, Vaulot D *et al.* Enumeration of phytoplankton, bacteria, and viruses in
772 marine samples. *Curr Protoc Cytom* 1999;**10**:11.11.1-11.11.15.

773 Meiners K, Gradinger R, Fehling J *et al.* Vertical distribution of exopolymer particles in sea ice
774 of the Fram Strait (Arctic) during autumn. *Mar Ecol Prog Ser* 2003;**248**:1–13.

775 Meiners K, Krembs C, Gradinger R. Exopolymer particles: microbial hotspots of enhanced
776 bacterial activity in Arctic fast ice (Chukchi Sea). *Aquat Microb Ecol* 2008;**52**:195–207.

777 Michel C, Nielsen T, Nozais C *et al.* Significance of sedimentation and grazing by ice micro-
778 and meiofauna for carbon cycling in annual sea ice (northern Baffin Bay). *Aquat Microb*
779 *Ecol* 2002;**30**:57–68.

780 Molina- Santiago C, Udaondo Z, Gómez- Lozano M *et al.* Global transcriptional response of
781 solvent-sensitive and solvent-tolerant *Pseudomonas putida* strains exposed to toluene.
782 *Env Microbiol* 2017;**19**:645–58.

783 Muyzer G, de Waal EC, Uitterlinden AG. Profiling of complex microbial populations by
784 denaturing gradient gel electrophoresis analysis of polymerase chain reaction-amplified
785 genes coding for 16S rRNA. *Appl Environ Microbiol* 1993;**59**:695–700.

786 Nelson JR. Phytoplankton pigments in macrozooplankton feces: variability in carotenoid
787 alterations. *Mar Ecol Prog Ser* 1989;**52**:129–44.

788 Nichols PD, Skerratt JH, Davidson A *et al.* Lipids of cultured *Phaeocystis pouchetii*: Signatures
789 for food-web, biogeochemical and environmental studies in Antarctica and the Southern
790 ocean. *Phytochemistry* 1991;**30**:3209–14.

791 Okuyama H, Okajima N, Sasaki S *et al.* The *cis-trans* isomerization of the double bond of a
792 fatty acid as a strategy for adaptation to changes in ambient temperature in the
793 psychrophilic bacterium, *Vibrio* sp. strain ABE-1. *Biochim Biophys Acta* 1991;**1084**:13–
794 20.

795 Parsons T, Maita Y, Lalli C. A manual of chemical and biological methods for seawater
796 analysis. Pergamon, Oxford sized algae and natural seston size fractions. *Mar Ecol Prog*
797 *Ser* 1984;**199**:43–53.

798 Passow U. Transparent exopolymer particles (TEP) in aquatic environments. *Prog Oceanogr*
799 2002;**55**:287–333.

800 Perrette M, Yool A, Quartly GD *et al.* Near-ubiquity of ice-edge blooms in the Arctic.
801 *Biogeosciences* 2011;**8**:515–24.

802 Piuri M, Sanchez- Rivas C, Ruzal SM. Adaptation to high salt in *Lactobacillus*: role of peptides
803 and proteolytic enzymes. *J Appl Microbiol* 2003;**95**:372–9.

804 von Quillfeldt CH, Ambrose WG, Clough LM. High number of diatom species in first-year ice
805 from the Chukchi Sea. *Polar Biol* 2003;**26**:806–18.

806 Rampen SW, Abbas BA, Schouten S *et al.* A comprehensive study of sterols in marine diatoms
807 (Bacillariophyta): Implications for their use as tracers for diatom productivity. *Limnol*
808 *Oceanogr* 2010;**55**:91–105.

809 Riebesell U, Schloss I, Smetacek V. Aggregation of algae released from melting sea ice:
810 implications for seeding and sedimentation. *Polar Biol* 1991;**11**:239–48.

811 Riedel A, Michel C, Gosselin M. Seasonal study of sea-ice exopolymeric substances on the
812 Mackenzie shelf: implications for transport of sea-ice bacteria and algae. *Aquat Microb*
813 *Ecol* 2006;**45**:195–206.

814 Riisgaard K, Nielsen T, Hansen P. Impact of elevated pH on succession in the Arctic spring
815 bloom. *Mar Ecol Prog Ser* 2015;**530**:63–75.

816 Rontani J, Amiraux R, Lalande C *et al.* Use of palmitoleic acid and its oxidation products for
817 monitoring the degradation of ice algae in Arctic waters and bottom sediments. *Org*
818 *Geochem* 2018;**124**:88–102.

819 Rontani J, Charriere B, Petit M *et al.* Degradation state of organic matter in surface sediments
820 from the Southern Beaufort Sea: a lipid approach. *Biogeosciences* 2012;**9**:3513–30.

821 Rontani J-F, Belt ST, Brown TA *et al.* Monitoring abiotic degradation in sinking versus
822 suspended Arctic sea ice algae during a spring ice melt using specific lipid oxidation
823 tracers. *Org Geochem* 2016;**98**:82–97.

824 Salcher M, Pernthaler J, Psenner R *et al.* Succession of bacterial grazing defense mechanisms
825 against protistan predators in an experimental microbial community. *Aquat Microb Ecol*
826 2005;**38**:215–29.

827 Sameoto DD. Vertical distribution of zooplankton biomass and species in northeastern Baffin
828 Bay related to temperature and salinity. *Polar Biol* 1984;**2**:213–24.

829 Sazhin AF, Romanova ND, Kopylov AI *et al.* Bacteria and Viruses in Arctic Sea Ice.
830 *Oceanology* 2019;**59**:339–46.

831 Schlitzer R. *Ocean Data View.*, 2015.

832 Shin SY, Bajpai VK, Kim HR *et al.* Antibacterial activity of bioconverted eicosapentaenoic
833 (EPA) and docosahexaenoic acid (DHA) against foodborne pathogenic bacteria. *Int J*
834 *Food Microbiol* 2007;**113**:233–6.

835 Sicre M-A, Paillasseur J-L, Marty J-C *et al.* Characterization of seawater samples using
836 chemometric methods applied to biomarker fatty acids. *Org Geochem* 1988;**12**:281–8.

837 Simon M, Azam F. Protein content and protein synthesis rates of planktonic marine bacteria.
838 *Mar Ecol Prog Ser* 1989;**51**:201–13.

839 Simon M, Grossart H, Schweitzer B *et al.* Microbial ecology of organic aggregates in aquatic
840 ecosystems. *Aquat Microb Ecol* 2002;**28**:175–211.

841 Sinensky M. Homeoviscous adaptation-a homeostatic process that regulates the viscosity of
842 membrane lipids in *Escherichia coli*. *Proc Natl Acad Sci USA* 1974;**71**:522–5.

843 Smith D, Azam F. A simple, economical method for measuring bacterial protein synthesis rates
844 in seawater using ³H-leucine. *Mar Microb Food Web* 1992;**6**:107–14.

845 Smith SD, Muench RD, Pease CH. Polynyas and leads: An overview of physical processes and
846 environment. *J Geophys Res Oceans* 1990;**95**:9461–79.

847 Søreide JE, Leu E, Berge J *et al.* Timing of blooms, algal food quality and *Calanus glacialis*
848 reproduction and growth in a changing Arctic. *Glob Change Biol* 2010;**16**:3154–63.

849 Takai K, Horikoshi K. Rapid Detection and Quantification of Members of the Archaeal
850 Community by Quantitative PCR Using Fluorogenic Probes. *Appl Environ Microbiol*
851 2000;**66**:5066–72.

852 Thompson J, MacLeod R. Functions of Na⁺ and K⁺ in the active transport of α -aminoisobutyric
853 acid in a marine Pseudomonad. *J Biol Chem* 1971;**246**:4066–74.

854 Thornton DCO. Diatom aggregation in the sea: mechanisms and ecological implications. *Euro*
855 *J Phycol* 2002;**37**:149–61.

856 Tolosa I, Vescovali I, LeBlond N *et al.* Distribution of pigments and fatty acid biomarkers in
857 particulate matter from the frontal structure of the Alboran Sea (SW Mediterranean Sea).
858 *Mar Chem* 2004;**88**:103–25.

859 Wadhams P, Martin S. *Ice in the Ocean*. 2nd ed. CRC press, 2001.

860 Wakeham SG, Lee C. Organic geochemistry of particulate matter in the ocean: The role of
861 particles in oceanic sedimentary cycles. *Org Geochem* 1989;**14**:83–96.

862 Welschmeyer NA, Lorenzen CJ. Role of herbivory in controlling phytoplankton abundance:
863 annual pigment budget for a temperate marine fjord. *Mar Biol* 1985;**90**:75–86.

864

865

866 **Figure captions**

867

868 **Figure 1.** Map of the study area with location of the stations investigated in Baffin Bay. Blue
869 circles on the enlarged map of western Baffin Bay indicate the stations investigated during the
870 transect. The orange circle indicates the GreenEdge ice camp station investigated by Amiraux
871 et al. (2019, 2021a). White color indicates the sea ice cover during the sampling.

872 **Figure 2.** Chlorophyll *a* (A), phaeopigments (B) and total particulate carbon (C) in seawater at
873 the different stations investigated. Data were interpolated and plotted using Ocean Data View
874 v4.7.8 (Schlitzer, 2015).

875 **Figure 3.** Bacterial abundance (BA) (A) and bacterial production (BP) (B) in seawater at the
876 different stations investigated. Data were interpolated and plotted using Ocean Data View
877 v4.7.8 (Schlitzer, 2015).

878 **Figure 4.** Relative proportion of the main monounsaturated fatty acids (FA) and alcohols (ol)
879 in sea ice and underlying seawater at the different stations investigated.

880 **Figure 5.** Relative proportions of brassicasterol, desmosterol, sitosterol and 24-
881 methylenecholesterol in sea ice and underlying water column at the different stations
882 investigated.

883 **Figure 6.** MRM chromatograms (m/z 217 \rightarrow 185 and m/z 245 \rightarrow 213) of DMDS derivatives of
884 MUFAs in the bottommost layer of ice (0-3 cm) at St 409.

885 **Figure 7.** Mean *Trans/cis* ratio of vaccenic (C_{18:1Δ11}), oleic (C_{18:1Δ9}), and hexadec-11-enoic
886 (C_{16:1Δ11}) acids in sea ice and the underlying water column at the different stations investigated

887 (n = 3, analytical triplicates). For each station and each acid, significantly different values are
888 annotated with different letters (P < 0.05).

889 **Figure 8.** Conceptual scheme summarizing the main results obtained.

890

891 **Table 1.** Mean percentage of dead attached bacteria in sea ice and SPM samples collected at St
892 409 and St 418 (n = 3, 2 samples + an analytical replicate). For each station, significantly
893 different values are annotated with different letters (P < 0.05).

894

895

896 **Supplementary material**

897

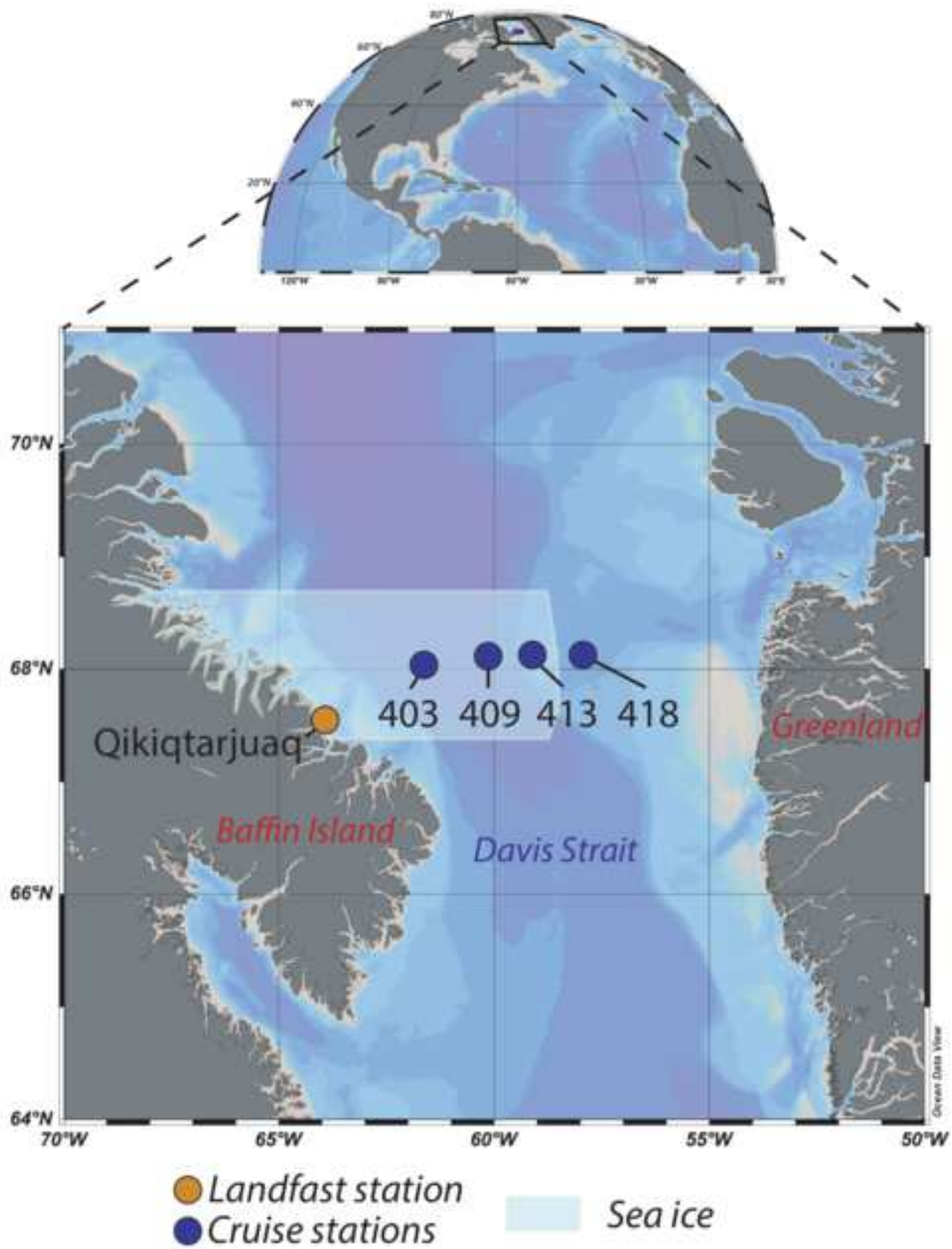
898 **Fig. S1:** Concentrations (number of individuals per m³) of dominant copepod species at the
899 different stations investigated, according to their development stages. Main feeding modes are
900 indicated -her: herbivorous, -omn: omnivorous, -car: carnivorous. Herbivorous species, and
901 young development stages in particular, show high variations in abundances along sea ice
902 gradients, while it is less clear for omnivorous species.

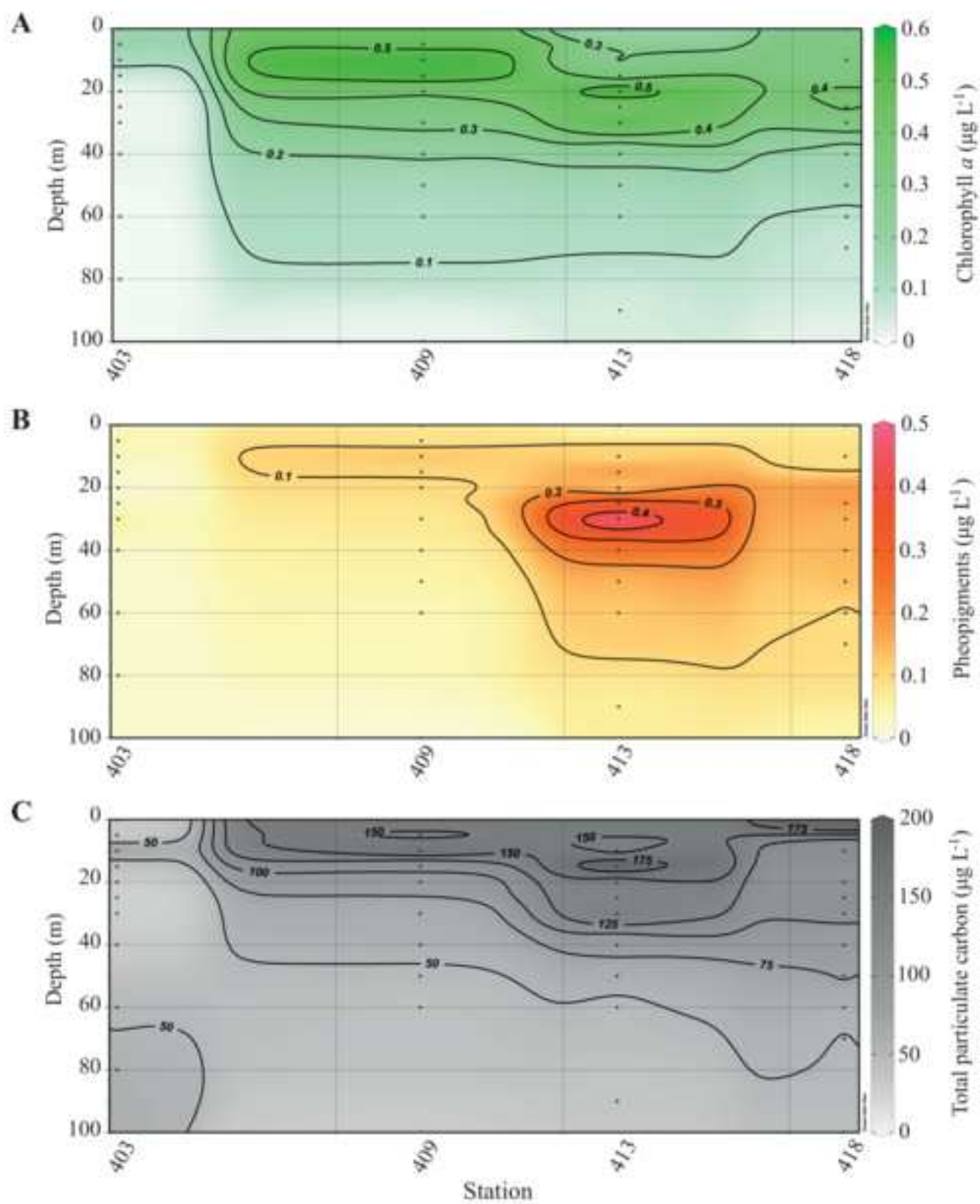
903

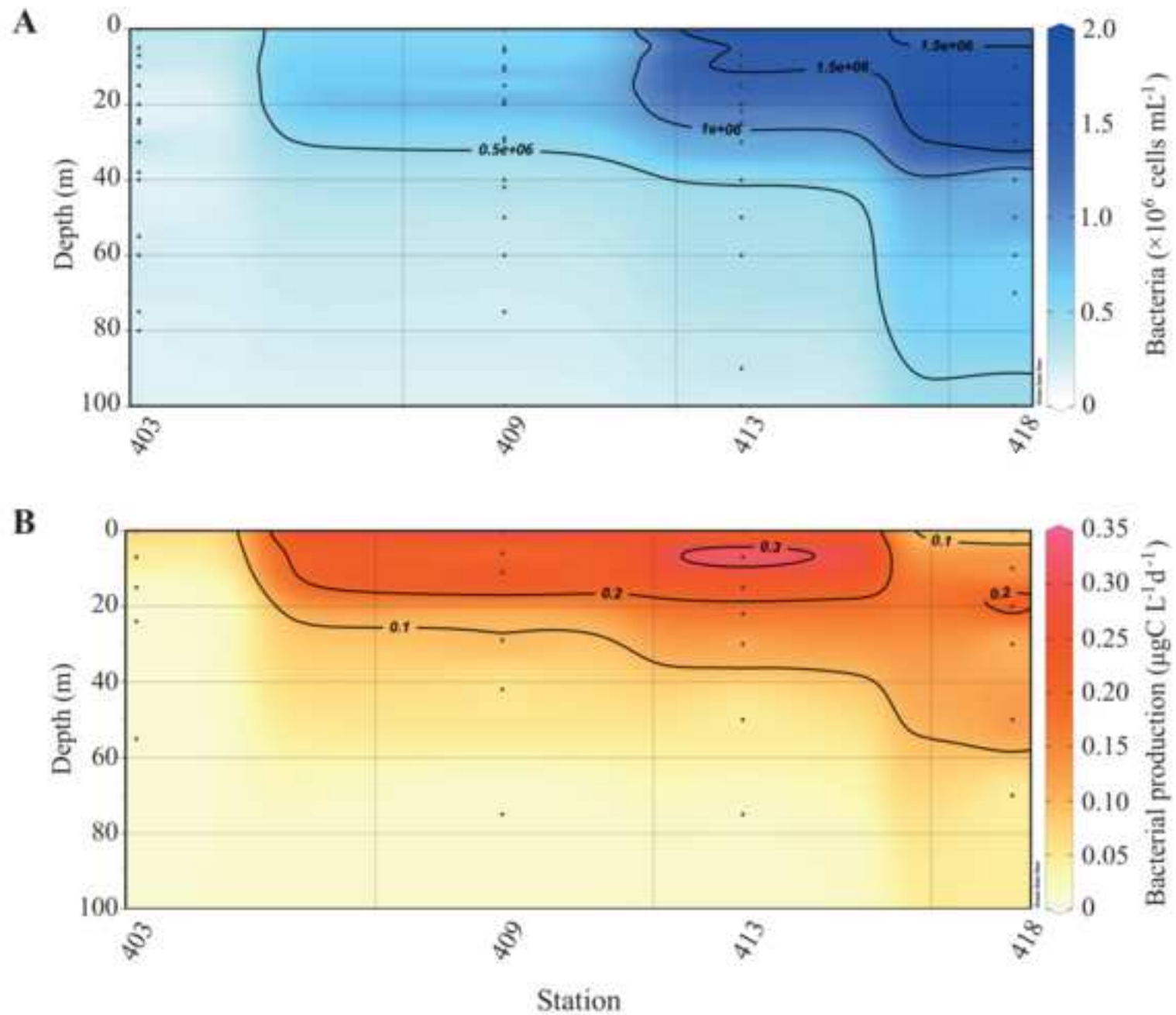
Table 1

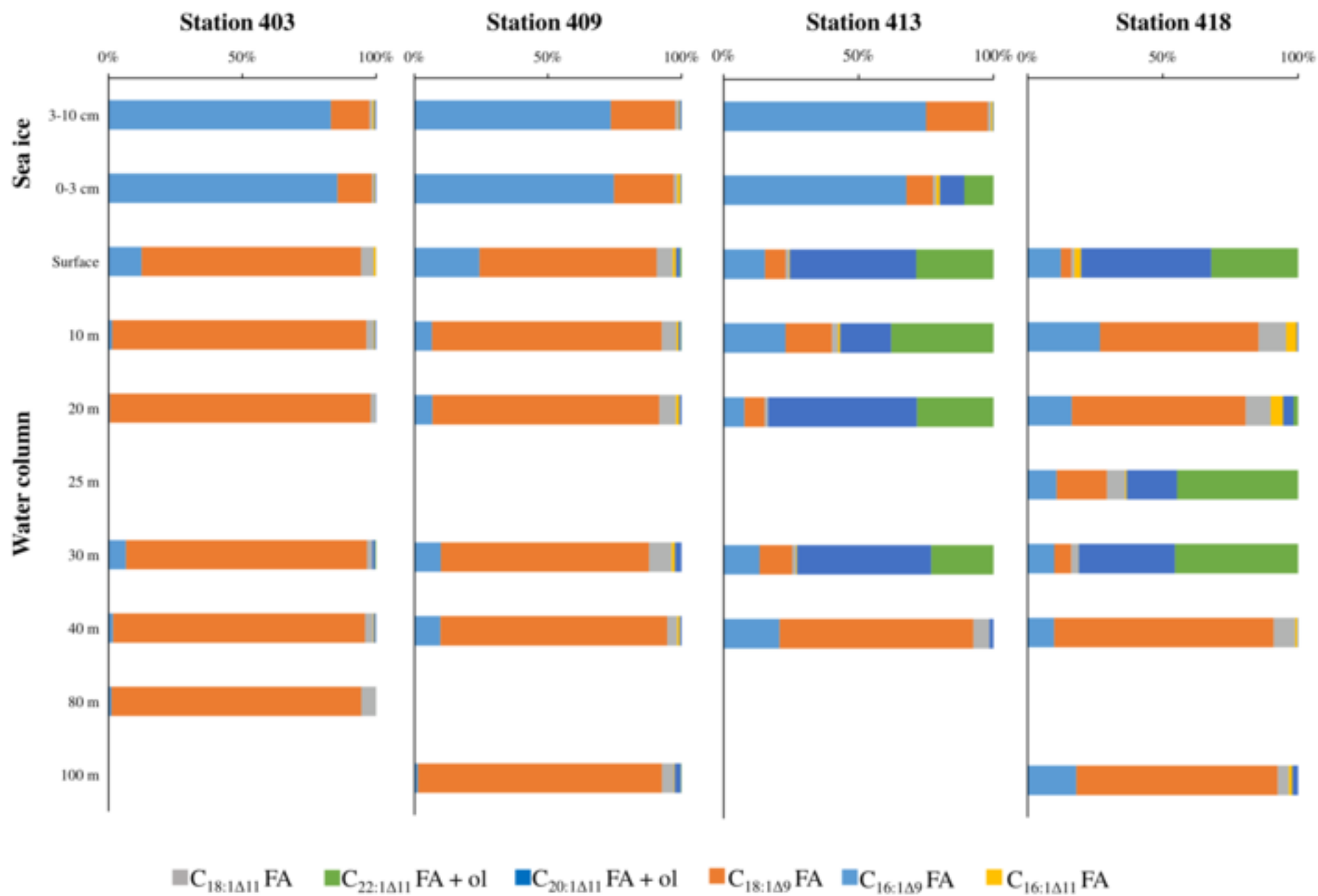
Mean percentage of dead attached bacteria in sea ice and SPM samples collected at St 409 and St 418 (n = 3). For each station, significantly different values are annotated with different letters (P < 0.05).

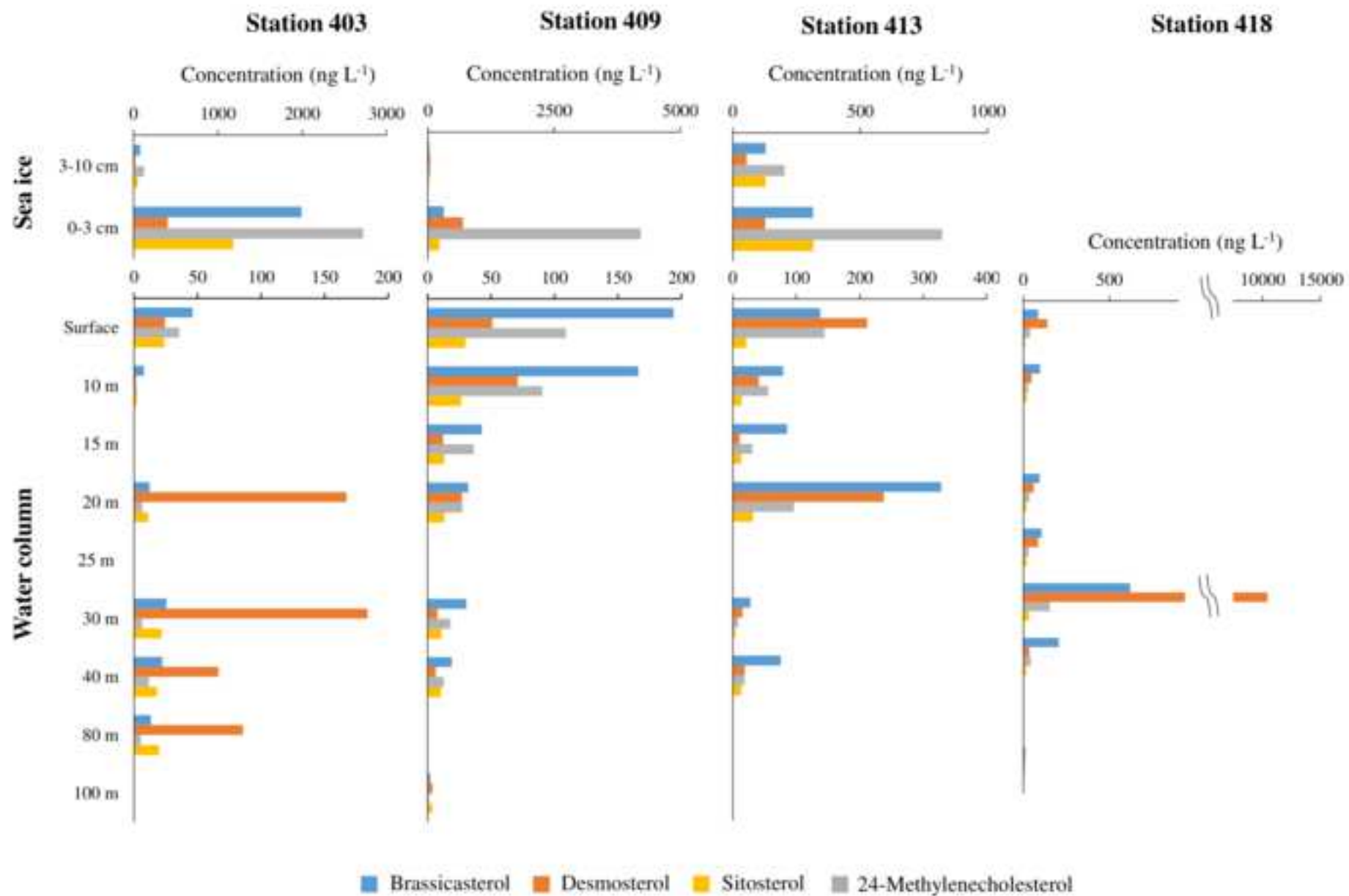
Station	Sample	Dead bacteria (%)
St 409	Ice (3-10 cm)	88.7 ± 4.7 (b)
St 409	Ice (0-3 cm)	84.3 ± 9.7 (b)
St 409	SPM 10 m	62.3 ± 22.06 (ab)
St 409	SPM 20 m	0 ± 11.9 (a)
St 418	SPM surface	23.3 ± 11.3 (b)
St 418	SPM 20 m	67.5 ± 4.1 (c)
St 418	SPM 30 m	3.8 ± 39.0 (ab)
St 418	SPM 40 m	0.6 ± 15.5 (ab)
St 418	SPM 100 m	0 ± 4.6 (a)

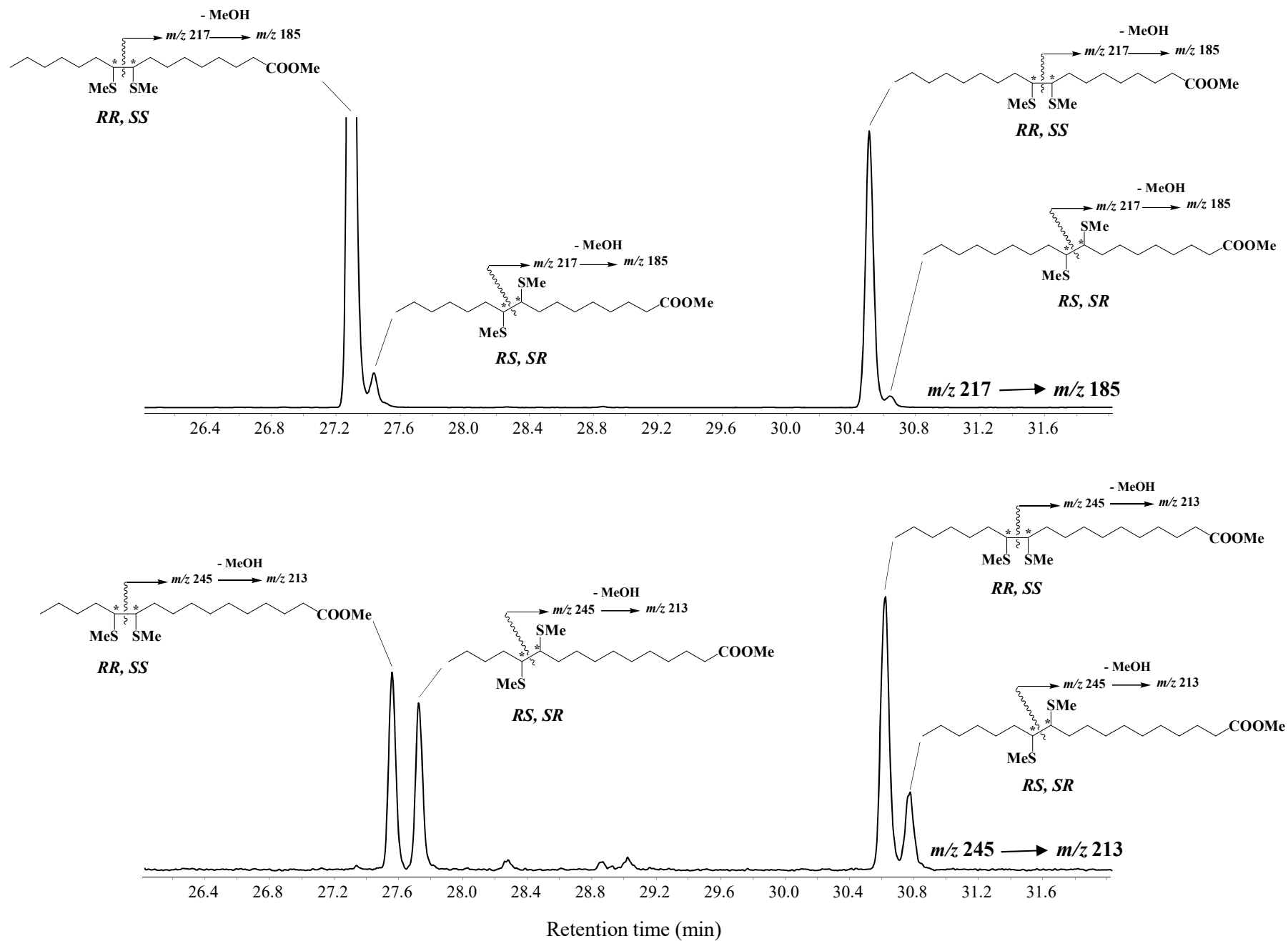


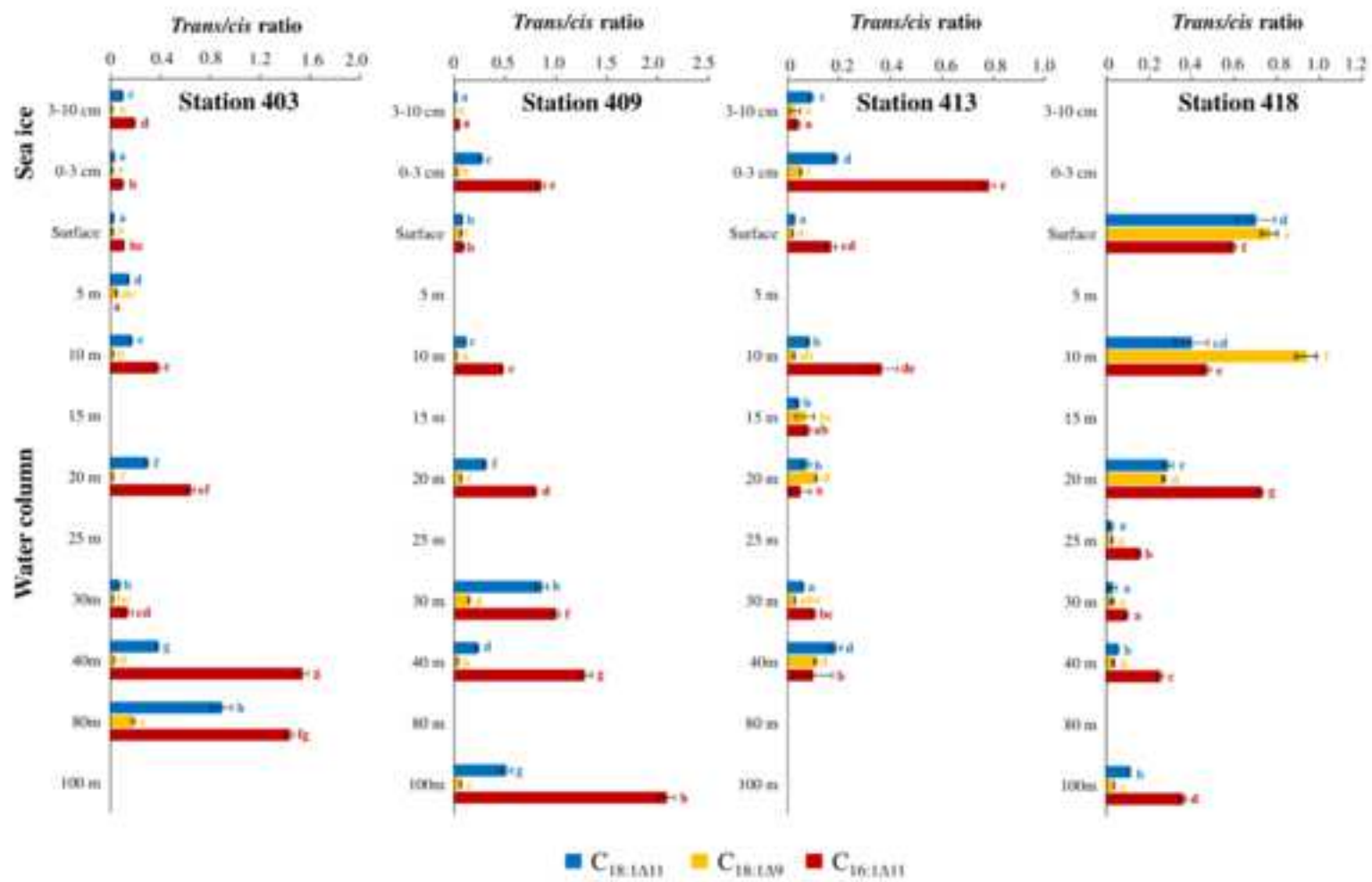


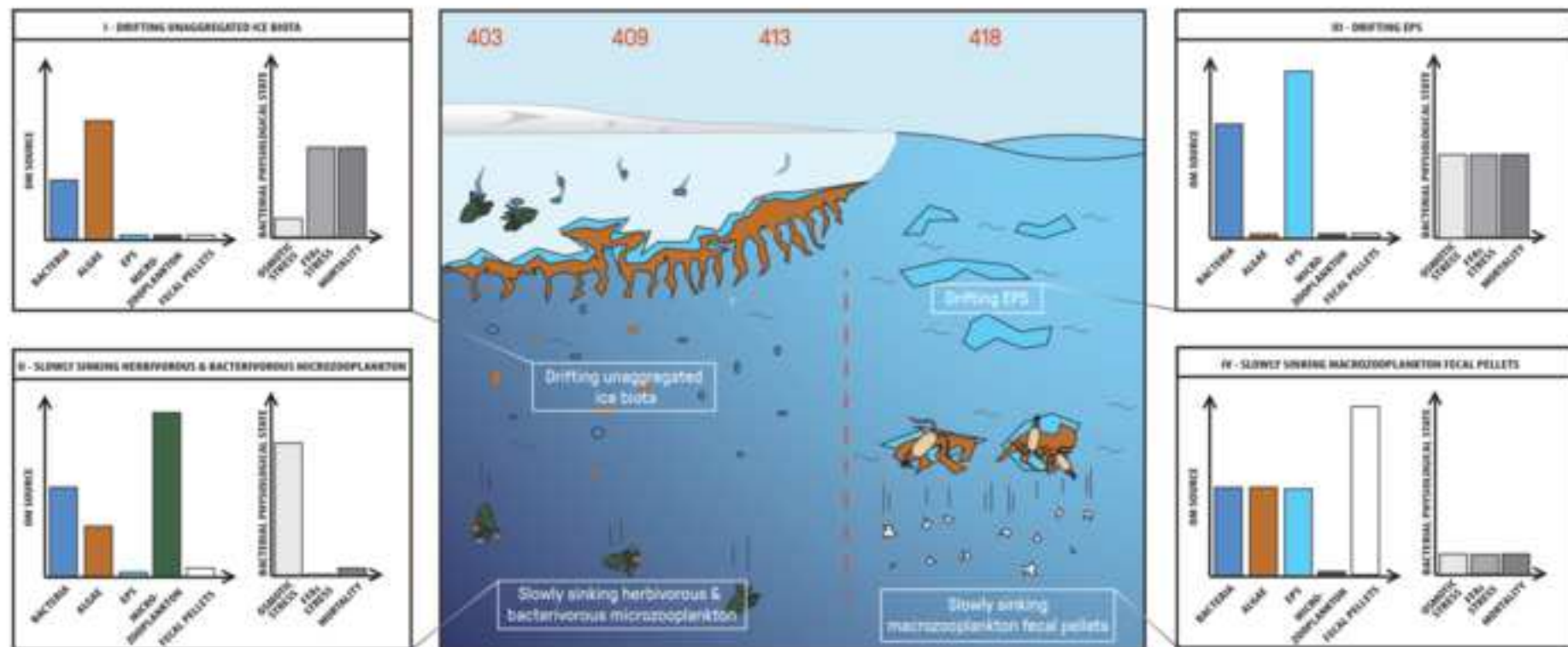








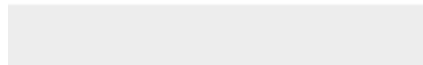






[Click here to access/download](#)

Supplementary material for on-line publication only
Supp Fig S1.tiff



Author contributions:

- Burot C. Investigation (lipid tracers and molecular biology), writing
- Amiraux R. Investigation (lipid tracers), writing, resources
- Bonin P. Conceptualization, writing, methodology
- Guasco S. Investigation (Molecular biology)
- Babin M. Funding acquisition, writing
- Joux F. Investigation (bacterial production)
- Marie D. Investigation (bacterial numeration)
- Vilgrain L. Investigation (zooplankton), writing
- Heipieper H. Writing
- Rontani J.-F. Conceptualization, writing, methodology, funding acquisition

Declaration of interests

The authors declare that they have no known competing financial interests or personal relationships that could have appeared to influence the work reported in this paper.

The authors declare the following financial interests/personal relationships which may be considered as potential competing interests: